A&A 442, 11–28 (2005)
DOI: 10.1051/0004-6361:20042493

Astronomy & Astrophysics

Stochastic polarized line formation

I. Zeeman propagation matrix in a random magnetic field⋆

H. Frisch[1], M. Sampoorna[1,2,3], and K. N. Nagendra[1,2]

[1] Laboratoire Cassiopée (CNRS, UMR 6202), Observatoire de la Côte d'Azur, BP 4229, 06304 Nice Cedex 4, France
[2] Indian Institute of Astrophysics, Koramangala Layout, Bangalore 560 034, India
[3] JAP, Dept. of Physics, Indian Institute of Science, Bangalore 560 012, India

Received 7 December 2004 /Accepted 4 July 2005

ABSTRACT

This paper considers the effect of a random magnetic field on Zeeman line transfer, assuming that the scales of fluctuations of the random field are much smaller than photon mean free paths associated to the line formation (micro-turbulent limit). The mean absorption and anomalous dispersion coefficients are calculated for random fields with a given mean value, isotropic or anisotropic Gaussian distributions azimuthally invariant about the direction of the mean field. Following Domke & Pavlov (1979, Ap&SS, 66, 47), the averaging process is carried out in a reference frame defined by the direction of the mean field. The main steps are described in detail. They involve the writing of the Zeeman matrix in the polarization matrix representation of the radiation field and a rotation of the line of sight reference frame. Three types of fluctuations are considered : fluctuations along the direction of the mean field, fluctuations perpendicular to the mean field, and isotropic fluctuations. In each case, the averaging method is described in detail and fairly explicit expressions for the mean coefficients are established, most of which were given in Dolginov & Pavlov (1972, Soviet Ast., 16, 450) or Domke & Pavlov (1979, Ap&SS, 66, 47). They include the effect of a microturbulent velocity field with zero mean and a Gaussian distribution.
A detailed numerical investigation of the mean coefficients illustrates the two effects of magnetic field fluctuations: broadening of the σ-components by fluctuations of the magnetic field intensity, leaving the π-components unchanged, and averaging over the angular dependence of the π and σ components. For longitudinal fluctuations only the first effect is at play. For isotropic and perpendicular fluctuations, angular averaging can modify the frequency profiles of the mean coefficients quite drastically with the appearance of an unpolarized central component in the diagonal absorption coefficient, even when the mean field is in direction of the line of sight. A detailed comparison of the effects of the three types of fluctuation coefficients is performed. In general the magnetic field fluctuations induce a broadening of the absorption and anomalous dispersion coefficients together with a decrease of their values. Two different regimes can be distinguished depending on whether the broadening is larger or smaller than the Zeeman shift by the mean magnetic field.
For isotropic fluctuations, the mean coefficients can be expressed in terms of generalized Voigt and Faraday-Voigt functions $H^{(n)}$ and $F^{(n)}$ introduced by Dolginov & Pavlov (1972, Soviet Ast., 16, 450). These functions are related to the derivatives of the Voigt and Faraday-Voigt functions. A recursion relation is given in an Appendix for their calculation. A detailed analysis is carried out of the dependence of the mean coefficients on the intensity and direction of the mean magnetic field, on its root mean square fluctuations and on the Landé factor and damping parameter of the line.

Key words. line: formation – polarization – magnetic fields – turbulence – radiative transfer

1. Introduction

Observations of the solar magnetic field and numerical simulations of solar magneto-hydrodynamical processes all converge to a magnetic field which is highly variable on all scales, certainly in the horizontal direction and probably also in the vertical one. Solving radiative transfer equations for polarized radiation in a random magnetic field, is thus an important but not a simple problem since one is faced with a transfer equation with stochastic coefficients (Landi Degl'Innocenti 2003; Landi Degl'Innocenti & Landolfi 2004, henceforth LL04). In principle the mean radiation field can be found by numerical averaging over a large number of realizations of the magnetic field and other relevant random physical parameters like velocity and temperature. A more appealing approach is to construct, with chosen magnetic field models, closed form equations or expressions for the mean Stokes parameters. Landi Degl'Innocenti (2003) has given a nice and comprehensive review of the few models that have been proposed.

The problem of obtaining mean Stokes parameters simplifies if one can single out fluctuations with scales much smaller than the photon mean free paths. The radiative transfer equation

⋆ Appendices are only available in electronic form at
http://www.edpsciences.org

has the same form as in the deterministic case, except that the coefficients in the equation, in particular the absorption matrix, are replaced by averages over the distribution of the magnetic field vector and other relevant physical parameters. This microturbulent approximation is currently being used for diagnostic purposes in the frame work of the MISMA (Micro Structured Magnetic Atmospheres) hypothesis (Sánchez Almeida et al. 1996; Sánchez Almeida 1997; Sánchez Almeida & Lites 2000) and commonly observed features like Stokes V asymmetries and broad-band circular polarization could be correctly reproduced. In the MISMA modeling the mean Zeeman absorption matrix is actually a weighted sum of two or three absorption matrices, each corresponding to a different constituent of the atmosphere characterized by its physical parameters (filling factor, magnetic field intensity and direction, velocity field, etc.).

The problem simplifies also when the scales of fluctuations is much larger than the photon mean free-paths. The magnetic field can then be taken constant over the line forming region and the transfer equation for polarized radiation is the standard deterministic one. Mean Stokes parameters can be obtained by averaging its solution over the magnetic field distribution. For magnetic fields with a finite correlation length, i.e. comparable to photons mean free paths, the macroturbulent and microtubulent limits are recovered when the correlation scales go to infinity or zero.

The microturbulent limit is certainly a rough approximation to describe the effects of a random magnetic field, but as the small scale limit of more general models, it is interesting to study somewhat systematically the effect of a random magnetic field on the Zeeman absorption matrix. This is the main purpose of this paper. The problem has actually been addressed fairly early by Dolginov & Pavlov (1972, henceforth DP72) and by Domke & Pavlov (1979, henceforth DP79), with anisotropic Gaussian distributions of the magnetic field vector. These two papers have attracted very little attention, although they contain quite a few interesting results showing the drastic effects of isotropic or anisotropic magnetic field distributions with a non zero mean field. More simple distribution have been introduced for diagnostic purposes, in particular in relation with the Hanle effect. For example, following Stenflo (1982), a single-valued magnetic field with isotropic distribution is commonly used to infer turbulent magnetic fields from the linear polarization of Hanle sensitive lines (Stenflo 1994; Faurobert-Scholl 1996, and references therein). A somewhat more sophisticated model is worked out in detail in LL04 for the case of the Zeeman effect. The angular distribution is still isotropic, but the field modulus has a Gaussian distribution with zero mean. The two models predict zero polarization for the Zeeman effect since all the off diagonal elements of the absorption matrix are zero. Recently, measurements of the fractal dimensions of magnetic structures in high-resolution magnetograms and numerical simulations of magneto-convection have suggested that the distribution of the modulus of the magnetic and of the vertical component could be described by stretched exponentials (Cattaneo 1999; Stenflo & Holzreuter 2002; Cattaneo et al. 2003; Janßen et al. 2003). Such distributions are now considered for diagnostic purposes (Socas-Navarro & Sánchez Almeida 2003; Trujillo Bueno et al. 2004). Actually not so much is known on the small scale distribution of the magnetic field vector and on the correlations between the magnetic field and velocity field fluctuations. For isotropic turbulence, symmetry arguments give that they are zero when the magnetic field is treated as a pseudovector (DP79).

Here we concentrate on the effects of Gaussian magnetic field fluctuations. We believe that a good understanding of the sole action of a random magnetic field is important before considering more complex situations with anisotropic random velocity fields and correlations between velocity field and magnetic field fluctuations, although they seem to be needed to explain circular polarization asymmetries. One can find in LL04 (Chap. 9) a simple example showing the effects of such correlations. So here we assume, as in DP79, that there is no correlation between the magnetic field and velocity field fluctuations and that the latter behave like thermal velocity field fluctuations. They can thus be incorporated in the line Doppler width. We assume that the medium is permeated by a mean magnetic field $\boldsymbol{\mathcal{H}}_{\rm o}$ with anisotropic Gaussian fluctuations. We write the random field distribution function in the form

$$P(\boldsymbol{\mathcal{H}})\mathrm{d}\boldsymbol{\mathcal{H}} = \frac{1}{(2\pi)^{3/2}\sigma_{\rm T}^2\sigma_{\rm L}} \times \exp\left[-\frac{\mathcal{H}_{\rm T}^2}{2\sigma_{\rm T}^2}\right]\exp\left[-\frac{(\mathcal{H}_{\rm L}-\mathcal{H}_{\rm o})^2}{2\sigma_{\rm L}^2}\right]\mathrm{d}^2\mathcal{H}_{\rm T}\,\mathrm{d}\mathcal{H}_{\rm L}. \quad (1)$$

Here $\mathcal{H}_{\rm T}$ and $\mathcal{H}_{\rm L}$ are the components of the random field in the directions perpendicular and parallel to the mean field. The coefficient $\sigma_{\rm L}$ and $\sigma_{\rm T}$ are proportional to the root mean square (rms) fluctuations of the longitudinal and transverse components. With the above definition $\langle(\mathcal{H}_{\rm L}-\mathcal{H}_{\rm o})^2\rangle = \sigma_{\rm L}^2$ and $\langle\mathcal{H}_{\rm T}^2\rangle = 2\sigma_{\rm T}^2$. We will also consider the case of isotropic fluctuations with $\sigma_{\rm T} = \sigma_{\rm L} = \sigma$. In that case $\langle(\boldsymbol{\mathcal{H}}-\boldsymbol{\mathcal{H}}_{\rm o})^2\rangle = 3\sigma^2$. The distribution written in Eq. (1) is invariant under a rotation about the direction of the mean field and is normalized to unity. The choice of the factor 2 in the exponential is arbitrary. Changing it will modify the normalization constant and the relation between the rms fluctuations and the coefficients $\sigma_{\rm T}$ and $\sigma_{\rm L}$.

The distribution written in Eq. (1) is the most general azimuthally symmetric Gaussian distribution. Here we consider three specific types of fluctuations: (i) longitudinal fluctuations in the direction of the mean field, also referred to as 1D fluctuations; they correspond to the case $\sigma_{\rm T} = 0$; (ii) isotropic fluctuations, also referred to as 3D fluctuations; they correspond to $\sigma_{\rm T} = \sigma_{\rm L}$ (iii); fluctuations perpendicular to the mean field which we refer to as 2D fluctuations; they correspond to the case $\sigma_{\rm L} = 0$. In cases (i) and (iii) the fluctuations are anisotropic. They are isotropic by construction in case (ii). In case (i), only the magnitude of $\boldsymbol{\mathcal{H}}$ is random but in cases (ii) and (iii), both the amplitude and the direction of the magnetic field are random.

For these three types of distribution we give expressions, as explicit as possible, of the mean absorption and anomalous dispersion coefficients. Many of them can be found also in DP72 and DP79 where they are often stated with only a few hints at how they may be obtained. Here we give fairly detailed proofs. Some of them can be easily transposed to non-Gaussian distribution functions. Also we perform a much more extended

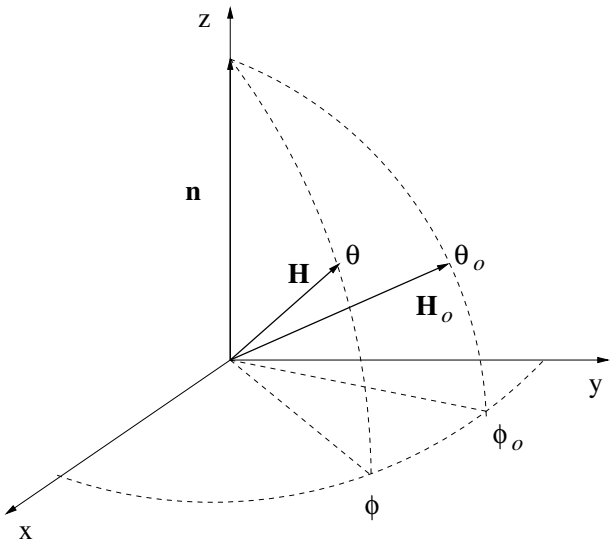

Fig. 1. Definition of θ and ϕ, the polar and azimuthal angles of the random magnetic field vector $\boldsymbol{\mathcal{H}}$, and of $\theta_{\rm o}$ and $\phi_{\rm o}$, the corresponding angles for the mean magnetic field $\boldsymbol{\mathcal{H}}_{\rm o}$.

numerical analysis of the mean coefficients and in particular carry out a detailed comparison of the frequency profiles produced by the longitudinal, perpendicular and isotropic distributions. This comparison is quite useful for building a physical insight into the averaging effects.

This paper is organized as follows. In Sect. 2 we establish a general expression for the calculation of the mean Zeeman absorption matrix which holds for any azimuthally invariant magnetic field vector distributions. In Sects. 3, 4 and 5 we consider in detail the three specific distributions listed above. Section 6 is devoted to a summary of the main results and contains also some comments on possible generalizations.

2. The Zeeman propagation matrix

We are interested in the calculation of

$$\langle\hat{\Phi}\rangle = \int \hat{\Phi}(\boldsymbol{\mathcal{H}})\, P(\boldsymbol{\mathcal{H}})\, {\rm d}\boldsymbol{\mathcal{H}}, \tag{2}$$

where $\hat{\Phi}$ is the propagation matrix in the transfer equation for polarized radiation. It depends on the modulus of the magnetic field $|\boldsymbol{\mathcal{H}}| = \mathcal{H}$ and on the angle between the line of sight (LOS) and the direction of the magnetic field. In the line LOS reference frame shown in Fig. 1 where the z-axis is toward the observer, $\hat{\Phi}$ depends on the polar and azimuthal angles θ and ϕ of the random magnetic field. In contrast, the magnetic field distribution introduced in Eq. (1) is defined with respect to the direction of the mean field $\boldsymbol{\mathcal{H}}_{\rm o}$. In terms of Θ and Ψ, the polar and azimuthal angles of $\boldsymbol{\mathcal{H}}$ with respect to $\boldsymbol{\mathcal{H}}_{\rm o}$, the distribution function has the form

$$P(\boldsymbol{\mathcal{H}}){\rm d}\boldsymbol{\mathcal{H}} = \frac{1}{(2\pi)^{3/2}\sigma_{\rm T}^2\sigma_{\rm L}} \exp\left[-\frac{\mathcal{H}^2\sin^2\Theta}{2\sigma_{\rm T}^2}\right] \times \exp\left[-\frac{(\mathcal{H}\cos\Theta - \mathcal{H}_{\rm o})^2}{2\sigma_{\rm L}^2}\right] \mathcal{H}^2\sin\Theta\,{\rm d}\mathcal{H}\,{\rm d}\Theta\,{\rm d}\Psi. \tag{3}$$

To carry out the averaging process, one must either express $P(\boldsymbol{\mathcal{H}})\,d\boldsymbol{\mathcal{H}}$ in terms of θ and ϕ or the matrix $\hat{\Phi}$ in terms of Θ and Ψ. The second option is actually simpler to work out. As pointed out in DP79, the angular dependence of the elements of $\hat{\Phi}$ can be written in terms of the spherical harmonics $Y_{lm}(\theta,\phi)$. This comes out naturally when the radiation field is represented by means of the polarization matrix rather than with the Stokes parameters. The Y_{lm}, because they are tensors of rank l, obey well known transformation laws under a rotation of the reference frame. A rotation of the LOS reference frame to a new frame defined by the direction of the mean magnetic field will thus yield the elements of $\hat{\Phi}$ in terms of Θ and Ψ. The averaging process can then be carried out fairly easily.

In Sect 2.1 we recall the standard expressions of the elements of the 4×4 Zeeman absorption matrix in the Stokes parameters representation and in Sect. 2.2 we give their expression in the polarization matrix representation. In Sect. 2.3 we explain in detail the transformation of the Y_{lm} and in Sect. 2.4 establish general expressions for the mean coefficients.

2.1. Absorption and anomalous dispersion coefficients

We consider for simplicity a normal Zeeman triplet but our results are easily generalized to the anomalous Zeeman effect (see Sect. 6). For a normal Zeeman triplet, the line absorption matrix can be written as (Landi Degl'Innocenti 1976; Rees 1987; Stenflo 1994; LL04)

$$\hat{\boldsymbol{\Phi}} = \begin{bmatrix} \varphi_I & \varphi_Q & \varphi_U & \varphi_V \\ \varphi_Q & \varphi_I & \chi_V & -\chi_U \\ \varphi_U & -\chi_V & \varphi_I & \chi_Q \\ \varphi_V & \chi_U & -\chi_Q & \varphi_I \end{bmatrix}. \tag{4}$$

The absorption coefficients, $\varphi_{I,Q,U,V}$ and the anomalous dispersion coefficients $\chi_{Q,U,V}$ may be written as

$$\begin{aligned}
\varphi_I &= \frac{1}{2}\varphi_0\sin^2\theta + \frac{1}{4}(\varphi_{+1}+\varphi_{-1})(1+\cos^2\theta),\\
\varphi_Q &= \frac{1}{2}\left[\varphi_0 - \frac{1}{2}(\varphi_{+1}+\varphi_{-1})\right]\sin^2\theta\cos2\phi,\\
\varphi_U &= \frac{1}{2}\left[\varphi_0 - \frac{1}{2}(\varphi_{+1}+\varphi_{-1})\right]\sin^2\theta\sin2\phi,\\
\varphi_V &= \frac{1}{2}(\varphi_{+1}-\varphi_{-1})\cos\theta,\\
\chi_Q &= \frac{1}{2}\left[f_0 - \frac{1}{2}(f_{+1}+f_{-1})\right]\sin^2\theta\cos2\phi,\\
\chi_U &= \frac{1}{2}\left[f_0 - \frac{1}{2}(f_{+1}+f_{-1})\right]\sin^2\theta\sin2\phi,\\
\chi_V &= \frac{1}{2}(f_{+1}-f_{-1})\cos\theta.
\end{aligned} \tag{5}$$

Here φ_q ($q = 0, \pm1$) are Voigt functions and f_q Faraday-Voigt functions defined below.

We introduce a Doppler width $\Delta_{\rm D}$ and measure all the independent variables appearing in φ_q and f_q in Doppler width units. We thus write

$$\begin{aligned}
\varphi_q(x,a,\mathcal{H}) &= H(x - q\Delta\mathcal{H}, a)\\
&= \frac{a}{\pi^{3/2}}\int_{-\infty}^{+\infty}\frac{{\rm e}^{-u^2}}{(x-q\Delta\mathcal{H}-u)^2+a^2}\,{\rm d}u,
\end{aligned} \tag{6}$$

and

$$f_q(x,a,\mathcal{H}) = F(x-q\Delta\mathcal{H},a) = \frac{1}{\pi^{3/2}}\int_{-\infty}^{+\infty}\frac{(x-q\Delta\mathcal{H}-u)\mathrm{e}^{-u^2}}{(x-q\Delta\mathcal{H}-u)^2+a^2}\,\mathrm{d}u, \quad (7)$$

where $x=(\nu-\nu_\mathrm{o})/\Delta_\mathrm{D}$ is the frequency measured from the line center, in units of Δ_D, a the damping parameter and $\Delta\mathcal{H}$ the Zeeman displacement by the random field with

$$\Delta = g\frac{e}{4\pi mc}\frac{1}{\Delta_\mathrm{D}}. \quad (8)$$

Here g is the Landé factor, c the velocity of light, m and e, the mass and charge of the electron.

We use here Voigt functions which are normalized to unity when integrated over the dimensionless frequency x, and the associated Faraday-Voigt functions (a factor $1/\sqrt{\pi}$ is added to the usual definition of H and a factor $2/\sqrt{\pi}$ to the usual definition of F). With this definition the Voigt function is exactly the convolution product of a Lorentzian describing the natural width of the line and of a Gaussian. The latter can describe pure thermal Doppler broadening, or a combination of thermal and microturbulent velocity broadening, provided the velocity field has an isotropic Maxwellian distribution. What we call here the Doppler width and denote by Δ_D is actually the total broadening parameter, including the microturbulent velocity field. Thus, with standard notations,

$$\Delta_\mathrm{D} = \frac{\nu_\mathrm{o}}{c}\left(v_\mathrm{th}^2+v_\mathrm{tv}^2\right)^{1/2}, \quad (9)$$

where ν_o is the line center frequency, $v_\mathrm{th}=(2kT/M)^{1/2}$ and v_tv are the root-mean-square thermal and turbulent velocities, respectively.

If the frequency x is measured in units of thermal Doppler width $\Delta_\mathrm{D} = \nu_\mathrm{o}v_\mathrm{th}/c$, then $\varphi_q(x,a)\mathrm{d}x$ become $\varphi_q(x/\gamma_\mathrm{v},a/\gamma_\mathrm{v})\mathrm{d}x/\gamma_\mathrm{v}$ with $\gamma_\mathrm{v}=(1+v_\mathrm{tv}^2/v_\mathrm{th}^2)^{1/2}$. The change of variables $x/\gamma_\mathrm{v}\rightarrow x$ and $a/\gamma_\mathrm{v}\rightarrow a$ and the definition of Δ_D as in Eq. (9) lead back to Eqs. (6) and (7).

2.2. A different form for the Zeeman matrix elements

For the calculation of the mean Zeeman propagation matrix, it is convenient to rewrite the elements as in DP79, namely in the form

$$\begin{aligned}\varphi_I &= A_0-\frac{1}{3}A_2(3\cos^2\theta-1),\\ \varphi_V &= A_1\cos\theta,\\ \varphi_Q &= A_2\sin^2\theta\cos 2\phi,\\ \varphi_U &= A_2\sin^2\theta\sin 2\phi,\end{aligned} \quad (10)$$

with

$$\begin{aligned}A_0 &= \frac{1}{3}\sum_{q=-1}^{q=+1}\varphi_q(x,a,\mathcal{H}),\quad q=0,\pm1\\ A_1 &= \frac{1}{2}\sum_{q=\pm1}q\varphi_q(x,a,\mathcal{H}),\\ A_2 &= \frac{1}{4}\sum_{q=-1}^{q=+1}(2-3q^2)\varphi_q(x,a,\mathcal{H}),\quad q=0,\pm1.\end{aligned} \quad (11)$$

The anomalous dispersion coefficients have similar expressions with the φ_q replaced by the f_q. It is straightforward to verify that the expressions given above are identical to those given in Eq. (5). We note here that they appear automatically when the polarized radiation field is represented by the time averaged polarization tensor rather than by the Stokes vector (DP72; DP79; Dolginov et al. 1995).

The main interest of this formulation, in addition to the fact that the A_i, $(i=0,1,2)$ depend only on the intensity of the random magnetic field, is that the functions which contain the angular dependence can be expressed in terms of spherical harmonics $Y_{l,m}(\theta,\phi)$ and Legendre polynomials $P_l(\cos\theta)$ which obey simple transformation laws in a rotation of the reference frame. In terms of these special functions,

$$\begin{aligned}\varphi_I &= A_0-\frac{2}{3}A_2P_2(\cos\theta)\\ \varphi_V &= A_1P_1(\cos\theta)\\ \varphi_Q &= \left(\frac{32\pi}{15}\right)^{1/2}A_2\frac{1}{2}[Y_{2,2}(\theta,\phi)+Y_{2,-2}(\theta,\phi)],\\ \varphi_U &= \left(\frac{32\pi}{15}\right)^{1/2}A_2\frac{1}{2}[Y_{2,2}(\theta,\phi)-Y_{2,-2}(\theta,\phi)].\end{aligned} \quad (12)$$

The Legendre polynomials $P_l(\cos\theta)$ are special cases of $Y_{lm}(\theta,\phi)$, corresponding to $m=0$ (see Appendix A).

2.3. Rotation of the reference frame

We now perform a rotation of the reference frame to obtain the absorption coefficients in a reference frame connected to the mean magnetic field where the averaging process is easily carried out. The initial reference frame is the (xyz) frame, also referred as the LOS reference frame (see Fig. 1). We perform on this reference frame a rotation defined by the Euler angles $\alpha=\phi_\mathrm{o}$, $\beta=\theta_\mathrm{o}$ and $\gamma=0$. This rotation is realized by performing a rotation by an angle θ_o around the y axis and a rotation by an angle ϕ_o around the initial z-axis. Since the random field is invariant under a rotation about the direction of the mean field, we have taken $\gamma=0$. Rotational transformations and Euler angles are described in many textbooks (Brink & Satchler 1968; Varshalovich et al. 1988; LL04).

The spherical harmonics Y_{lm} are irreducible tensors of rank l. They are particular cases of the Wigner $D^{(l)}_{mm'}(\alpha,\beta,\gamma)$ functions corresponding to $m=0$ or $m'=0$ (see Appendix A). In a rotation of the reference frame, defined by the Euler angles α,β,γ, they transform according to (Varshalovich et al. 1988, p. 141, Eq. (1))

$$Y_{lm}(\Theta,\Psi)=\sum_{m'}Y_{lm'}(\theta,\phi)D^{(l)}_{m'm}(\alpha,\beta,\gamma), \quad (13)$$

where θ and ϕ are the polar angles in the initial LOS coordinate system and Θ and Ψ the polar angles in the final mean magnetic coordinate system. Thus Θ and Ψ define the direction of the random field $\boldsymbol{\mathcal{H}}$ in the new reference frame.

Actually, we need the inverse transformation which will give us the $Y_{lm}(\theta,\phi)$ in terms of the $Y_{lm}(\Theta,\Psi)$. The inverse transformation is (Varshalovich et al. 1988, p. 74, Eq. (13))

$$Y_{lm}(\theta,\phi)=\sum_{m'}Y_{lm'}(\Theta,\Psi)D^{(l)}_{m'm}(0,-\theta_\mathrm{o},-\phi_\mathrm{o}). \quad (14)$$

The inverse transformation is obtained by performing the three elementary rotations in the reverse order and with the opposite rotation angles. Explicit expressions of the Y_{lm} and $D^{(l)}_{m'm}$ are given in Appendix A.

To calculate the mean coefficients $\langle\varphi_{I,Q,U,V}\rangle$ we have to integrate Eq. (12) over Ψ. Since the distribution function $P(\boldsymbol{\mathcal{H}})$ and the A_i, $(i = 0, 1, 2)$ are independent of Ψ (see Eqs. (3) and (11)), only the Y_{lm} have to be integrated over Ψ. When Eq. (14) is integrated over Ψ, only the term with $m' = 0$ will remain. For $m' = 0$ the $D^{(l)}_{m'm}$ reduce to Y_{lm} and the Y_{l0} to Legendre polynomials. Thus after integration, Eq. (14) reduces to

$$\frac{1}{2\pi}\int Y_{lm}(\theta,\phi)\mathrm{d}\Psi = P_l(\cos\Theta)Y_{lm}(-\theta_\mathrm{o},-\phi_\mathrm{o}). \tag{15}$$

We are now in the position to average Eq. (12).

2.4. Mean coefficients

Using Eq. (15) with $l = 2$, $m = 0$ for φ_I, $l = 1$, $m = 0$ for φ_V and $l = 2$, $m = \pm 2$ for φ_Q and φ_U, we obtain the very compact expressions

$$\begin{aligned}
\langle\varphi_I\rangle &= \bar{A}_0 - \frac{1}{3}\bar{A}_2(3\cos^2\theta_\mathrm{o} - 1),\\
\langle\varphi_V\rangle &= \bar{A}_1\cos\theta_\mathrm{o},\\
\langle\varphi_Q\rangle &= \bar{A}_2\sin^2\theta_\mathrm{o}\cos 2\phi_\mathrm{o},\\
\langle\varphi_U\rangle &= \langle\varphi_Q\rangle\tan 2\phi_\mathrm{o},
\end{aligned} \tag{16}$$

where

$$\begin{aligned}
\bar{A}_0 &= \langle A_0(x,a,\mathcal{H})\rangle,\\
\bar{A}_1 &= \langle A_1(x,a,\mathcal{H})\cos\Theta\rangle,\\
\bar{A}_2 &= \langle A_2(x,a,\mathcal{H})\frac{1}{2}(3\cos^2\Theta - 1)\rangle.
\end{aligned} \tag{17}$$

The notation $\langle\ \rangle$ represents an integration over Θ and $\mathcal{H}$ weighted by the azimuthal average of the magnetic field distribution. This result is quite general and can be used for any random field distribution, provided it is invariant in rotations about the mean magnetic field direction. We have similar expressions for the $\chi_{Q,U,V}$ with the φ_q replaced by the f_q. Since $\langle\varphi_U\rangle$ is simply related to $\langle\varphi_Q\rangle$, (see Eq. (16)) we do not consider it in the following.

With the distribution functions considered here (see Eqs. (1) or (3)), the mean coefficients have the same symmetry properties as the non random coefficients, namely $\langle\varphi_I\rangle$ and $\langle\varphi_Q\rangle$ are symmetric with respect to the line center $x = 0$ (they are even functions of x) and $\langle\varphi_V\rangle$ is antisymmetric (odd function of x). We stress also that the integrals of $\langle\varphi_I\rangle$ and $\langle\varphi_Q\rangle$ over frequency are not affected by turbulence. Hence if one consider only the integration over $x \geq 0$, the integral of $\langle\varphi_Q\rangle$ is zero and the integral of $\langle\varphi_I\rangle$ equal to 1/2.

3. Longitudinal fluctuations (1D turbulence)

When fluctuations are along the direction of the mean field $\boldsymbol{\mathcal{H}}_\mathrm{o}$, the distribution function for the random field can be written

$$P_\mathrm{L}(\boldsymbol{\mathcal{H}})\,\mathrm{d}\boldsymbol{\mathcal{H}} = \frac{1}{(2\pi)^{1/2}\sigma}\exp\left[-\frac{(\mathcal{H}-\mathcal{H}_\mathrm{o})^2}{2\sigma^2}\right]\mathrm{d}\mathcal{H}, \tag{18}$$

where $\mathcal{H}$ is the 1D random magnetic field which varies between $-\infty$ and $+\infty$ and $\sigma = [\langle(\mathcal{H}-\mathcal{H}_\mathrm{o})^2\rangle]^{1/2} = [\langle\mathcal{H}^2\rangle - \mathcal{H}_\mathrm{o}^2]^{1/2}$ is the square-root of the dispersion (or variance) around the mean field $\mathcal{H}_\mathrm{o}$, also known as the standard deviation or rms fluctuations. The factor 2 ensures that σ is exactly the rms fluctuation defined as above. This distribution is normalized to unity. It can be obtained from Eq. (1) by integrating over the transverse component of the magnetic field. To simplify the notation, we have set $\sigma_\mathrm{L} = \sigma$. We note that the Gaussian tends to a Dirac distribution when $\sigma \to 0$. Thus for $\sigma = 0$, the magnetic field is non-random and equal to the mean field $\boldsymbol{\mathcal{H}}_\mathrm{o}$.

We introduce the new dimensionless variable y and the parameters y_o and $\gamma_\mathcal{H}$ defined by

$$y = \frac{\mathcal{H}}{\sqrt{2}\sigma};\quad y_\mathrm{o} = \frac{\mathcal{H}_\mathrm{o}}{\sqrt{2}\sigma};\quad \gamma_\mathcal{H} = \Delta\sqrt{2}\sigma, \tag{19}$$

where the constant Δ is defined in Eq. (8). These dimensionless quantities will also be used in the case of isotropic and 2D turbulence. The variable y and the parameter y_o measure the random field and mean field in units of the standard deviation. The random Zeeman displacement is $\Delta\mathcal{H} = y\gamma_\mathcal{H}$ and the Zeeman shift by the mean field is $\Delta\mathcal{H}_\mathrm{o} = y_\mathrm{o}\gamma_\mathcal{H}$. In these new variables, φ_q can be written as

$$\varphi_q(x,a,y) = \frac{a}{\pi^{3/2}}\int_{-\infty}^{+\infty}\frac{\mathrm{e}^{-u^2}}{(x - q\gamma_\mathcal{H}y - u)^2 + a^2}\,\mathrm{d}u, \tag{20}$$

and the distribution function becomes

$$P_\mathrm{L}(\boldsymbol{\mathcal{H}})\,\mathrm{d}\boldsymbol{\mathcal{H}} = \frac{1}{\sqrt{\pi}}\,\mathrm{e}^{-(y-y_\mathrm{o})^2}\,\mathrm{d}y, \tag{21}$$

with y varying from $-\infty$ to $+\infty$.

To calculate the mean absorption coefficients it suffices to take the average of the A_i over $\mathcal{H}$ in Eq. (11) since the random field is along the direction θ_o, ϕ_o. This procedure is equivalent to set $\cos\Theta = 1$ in Eq. (17). The averaging over the magnetic field distribution amounts to the convolution product of a Voigt function with a Gaussian coming from the distribution of the magnetic field modulus. The effect is similar to a broadening by a Gaussian turbulent velocity field, except that it does not affect the φ_0 term (the π-component) since the latter does not depend on the modulus of the magnetic field. One obtains (see Appendix C)

$$\begin{aligned}
\bar{A}_0 &= \frac{1}{3}\sum_{q=-1}^{q=+1}\frac{1}{\gamma_q}H(\bar{x}_q,\bar{a}_q),\quad q = 0,\pm 1,\\
\bar{A}_1 &= \frac{1}{2}\sum_{q=\pm 1} q\frac{1}{\gamma_q}H(\bar{x}_q,\bar{a}_q),\\
\bar{A}_2 &= \frac{1}{4}\sum_{q=-1}^{q=+1}(2-3q^2)\frac{1}{\gamma_q}H(\bar{x}_q,\bar{a}_q),\quad q = 0,\pm 1,
\end{aligned} \tag{22}$$

where H is the Voigt function introduced in Eq. (6),

$$\bar{x}_q = \frac{x - q\Delta\mathcal{H}_\mathrm{o}}{\gamma_q},\quad \bar{a}_q = \frac{a}{\gamma_q}, \tag{23}$$

and

$$\gamma_q = \sqrt{1 + q^2\gamma_\mathcal{H}^2};\quad q = 0,\pm 1. \tag{24}$$

We see that γ_1 is a broadening parameter which combines the Doppler and magnetic field effects. Note that $\gamma_0 = 1$, $\bar{x}_0 = x$ and $\bar{a}_0 = a$. The φ_0 term is not modified as already mentioned above. Note also that the functions $H(\bar{x}_q, \bar{a}_q)/\gamma_q$ are normalized to unity (their integral over x is unity).

The broadening of the σ-components can be described in terms of a total Doppler width Δ_C that combines the effects of thermal, velocity and magnetic field broadening. It can be written as

$$\Delta_C = \sqrt{\Delta_D^2 + g^2 \left(\frac{e}{4\pi mc}\right)^2 2\sigma^2}, \tag{25}$$

where Δ_D is the Doppler width defined in Eq. (9).

When the Zeeman shift by the mean magnetic field $\Delta\mathcal{H}_o$ is smaller than the combined Doppler and magnetic broadening ($\Delta\mathcal{H}_o \ll \gamma_1$), a situation referred to as the *weak field limit*, as in DP72, one has, to the leading order

$$\begin{aligned}
\bar{A}_0 &\simeq \frac{1}{3}\left[H(x,a) + \frac{2}{\gamma_1} H\left(\frac{x}{\gamma_1}, \frac{a}{\gamma_1}\right)\right],\\
\bar{A}_1 &\simeq \frac{2\Delta\mathcal{H}_o}{\gamma_1^3}\left[xH\left(\frac{x}{\gamma_1}, \frac{a}{\gamma_1}\right) - aF\left(\frac{x}{\gamma_1}, \frac{a}{\gamma_1}\right)\right],\\
\bar{A}_2 &\simeq \frac{1}{2}\left[H(x,a) - \frac{1}{\gamma_1} H\left(\frac{x}{\gamma_1}, \frac{a}{\gamma_1}\right)\right].
\end{aligned} \tag{26}$$

When the mean field $\boldsymbol{\mathcal{H}}_o$ is zero, the circular polarization is zero but not the linear polarization unless the random field fluctuations are along the LOS ($\theta_o = 0°$). The mean diagonal absorption coefficient is given by

$$\langle\varphi_I\rangle = \frac{1}{2} H(x,a)\sin^2\theta_o + \frac{1}{2\gamma_1} H\left(\frac{x}{\gamma_1}, \frac{a}{\gamma_1}\right)(1 + \cos^2\theta_o). \tag{27}$$

To summarize, in the case of longitudinal fluctuations, the mean absorption coefficients have the same form as the original coefficients given in Eqs. (5) or (10) but the σ-components are broadened by the random magnetic field while the π-components are not affected. Mean coefficients for longitudinal fluctuations are shown in Sect. 5 and compared to the mean coefficients for 2D and 3D turbulence.

4. Isotropic fluctuations (3D turbulence)

We now assume that the fluctuations of the magnetic field are isotropically distributed. This implies that $\sigma_L = \sigma_T$ in Eq. (1). The distribution function takes the form

$$\begin{aligned}
P_I(\boldsymbol{\mathcal{H}})\,\mathrm{d}\boldsymbol{\mathcal{H}} &= \frac{1}{(2\pi)^{3/2}\sigma^3}\\
&\times \exp\left[-\frac{(\boldsymbol{\mathcal{H}} - \boldsymbol{\mathcal{H}}_o)^2}{2\sigma^2}\right] \mathcal{H}^2 \sin\Theta\,\mathrm{d}\mathcal{H}\,\mathrm{d}\Theta\,\mathrm{d}\Psi.
\end{aligned} \tag{28}$$

Here $\mathcal{H}$, the modulus of the magnetic field, varies from 0 to ∞. The rms fluctuations are $[\langle(\boldsymbol{\mathcal{H}} - \boldsymbol{\mathcal{H}}_o)^2\rangle]^{1/2} = [\langle\mathcal{H}^2\rangle - \mathcal{H}_o^2]^{1/2} = \sqrt{3}\sigma$. In terms of the dimensionless parameters introduced in Eq. (19), the distribution function becomes

$$P_I(\boldsymbol{\mathcal{H}})\,\mathrm{d}\boldsymbol{\mathcal{H}} = \frac{1}{\pi^{3/2}}\,\mathrm{e}^{-(y_o^2+y^2)}\,\mathrm{e}^{2y_o y\cos\Theta}\,y^2\,\mathrm{d}y\,\sin\Theta\,\mathrm{d}\Theta\,\mathrm{d}\Psi, \tag{29}$$

where y varies from 0 to ∞, the angle Θ from 0 to π and Ψ from 0 to 2π. The azimuthal average of this distribution is simply given by the rhs of Eq. (29) without the $\mathrm{d}\Psi$.

4.1. Exact and approximate expressions for the mean coefficients

We now calculate the $\bar{A}_i$ defined in Eq. (17). Introducing the variable $\mu = \cos\Theta$, we can write

$$\begin{aligned}
\bar{A}_i = \frac{2}{\sqrt{\pi}} \int_0^\infty \mathrm{e}^{-(y_o^2+y^2)} A_i(x, a, \sqrt{2}\sigma y) y^2\\
\times \int_{-1}^{+1} \mathrm{e}^{2y_o y\mu} c_i(\mu)\,\mathrm{d}\mu\,\mathrm{d}y,
\end{aligned} \tag{30}$$

where

$$c_0(\mu) = 1, \quad c_1(\mu) = \mu, \quad c_2(\mu) = \frac{1}{2}(3\mu^2 - 1). \tag{31}$$

The integration over μ can be carried out explicitly. Regrouping the exponential terms $\mathrm{e}^{-(y_o^2+y^2)}$ and $\mathrm{e}^{2y_o y}$ and then taking advantage of the symmetries with respect to a change y into $-y$, one obtains

$$\bar{A}_0 = \frac{2}{3\sqrt{\pi}} \sum_{q=-1}^{q=+1} \frac{1}{2y_o} \int_{-\infty}^{+\infty} \mathrm{e}^{-(y-y_o)^2} H(x - q\gamma_{\mathcal{H}} y, a) y\,\mathrm{d}y, \tag{32}$$

$$\begin{aligned}
\bar{A}_1 = \frac{1}{\sqrt{\pi}} \sum_{q=\pm1} q \frac{1}{2y_o} \int_{-\infty}^{+\infty} \mathrm{e}^{-(y-y_o)^2} H(x - q\gamma_{\mathcal{H}} y, a)\\
\times \left(y - \frac{1}{2y_o}\right) \mathrm{d}y,
\end{aligned} \tag{33}$$

$$\begin{aligned}
\bar{A}_2 = \frac{1}{2\sqrt{\pi}} \sum_{q=-1}^{q=+1} (2 - 3q^2) \frac{1}{2y_o} \int_{-\infty}^{+\infty} \mathrm{e}^{-(y-y_o)^2}\\
\times H(x - q\gamma_{\mathcal{H}} y, a) \left(y - \frac{3}{2y_o} + \frac{3}{4y_o^2 y}\right) \mathrm{d}y.
\end{aligned} \tag{34}$$

These equations, which are of the convolution type, were first given in DP79. Note that y varies from $-\infty$ to $+\infty$. For the anomalous dispersion coefficients we have similar relations where the Voigt functions H are replaced by the Faraday-Voigt functions F.

As shown in Appendix C, the $\bar{A}_i$ can be expressed in terms of the generalized Voigt and Faraday-Voigt functions $H^{(n)}$ and $F^{(n)}$ defined by

$$H^{(n)}(x,a) = \frac{a}{\pi^{3/2}} \int_{-\infty}^{+\infty} \frac{u^n \mathrm{e}^{-u^2}}{(x-u)^2 + a^2}\,\mathrm{d}u, \tag{35}$$

$$F^{(n)}(x,a) = \frac{1}{\pi^{3/2}} \int_{-\infty}^{+\infty} \frac{u^n (x-u) \mathrm{e}^{-u^2}}{(x-u)^2 + a^2}\,\mathrm{d}u. \tag{36}$$

They were introduced in DP72 were the $F^{(n)}$ are denoted $G^{(n)}$ (in DP79 they are denoted $Q^{(n)}$). For $n = 0$, one recovers the usual Voigt and Faraday-Voigt functions. The functions $H^{(n)}$ and $F^{(n)}$ are plotted in Fig. 2 for $a = 0$, $n = 0, 1, 2$. They can be calculated with recurrence relations given in Appendix D which take particularly simple forms for $a = 0$. In particular

$$H^{(n)}(x,0) = \frac{1}{\sqrt{\pi}} x^n \mathrm{e}^{-x^2}. \tag{37}$$

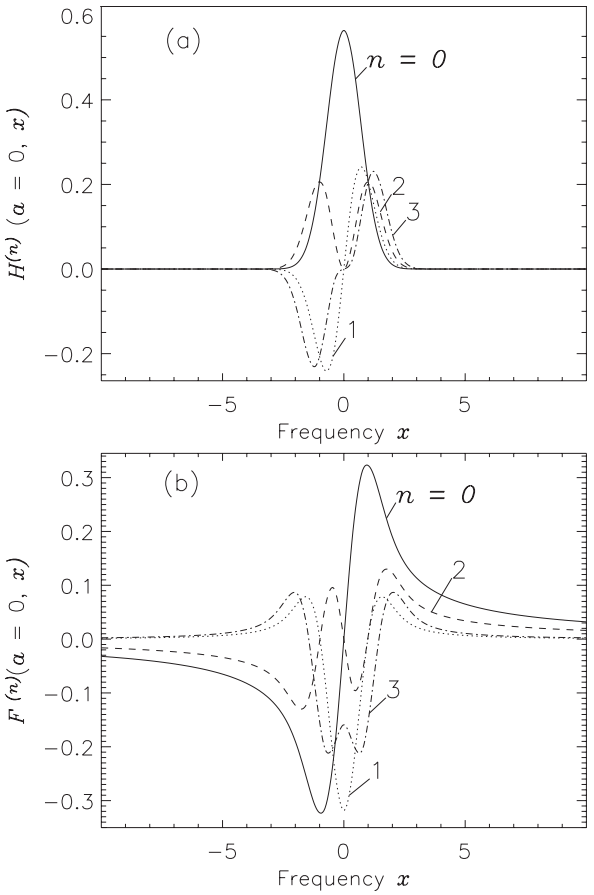

Fig. 2. The $H^{(n)}$ and $F^{(n)}$ functions for several orders n. The damping parameter $a = 0$. The $H^{(n)}$ are even functions when n is even and odd when n is odd. For the $F^{(n)}$ it is the opposite.

We also note that the $H^{(n)}$ and $F^{(n)}$ functions are simply related to the derivatives of the Voigt and Faraday-Voigt functions (see Appendix D).

The functions $\bar{A}_0$ and $\bar{A}_1$ have closed form (i.e. exact) expressions in terms of the $H^{(n)}$ but not $\bar{A}_2$ for which only approximate expressions can be given because of the term with $1/y$ (see Eq. (34)). The exact expressions for $\bar{A}_0$ and $\bar{A}_1$ are

$$\bar{A}_0 = \frac{1}{3}\sum_{q=-1}^{q=+1}\frac{1}{\gamma_q}\left[H^{(0)}(\bar{x}_q,\bar{a}_q) + q\frac{\gamma_{\mathcal{H}}}{y_o\gamma_q}H^{(1)}(\bar{x}_q,\bar{a}_q)\right], \tag{38}$$

$$\bar{A}_1 = \frac{1}{2}\sum_{q=\pm1} q\frac{1}{\gamma_q}\left[(1-\frac{1}{2y_o^2})H^{(0)}(\bar{x}_q,\bar{a}_q) + q\frac{\gamma_{\mathcal{H}}}{y_o\gamma_q}H^{(1)}(\bar{x}_q,\bar{a}_q)\right], \tag{39}$$

where $\bar{x}_q$ and $\bar{a}_q$ have been defined in Eq. (23).

For $\bar{A}_2$, approximate expressions can be constructed in the limiting cases $y_o \gg 1$ and $y_o \ll 1$, which we refer to respectively as the strong mean field and weak mean field limits for reasons explained now. We discuss these two cases separately.

4.1.1. Strong mean field limit

When the mean field intensity $\mathcal{H}_o$ is much larger than the rms fluctuations, i.e. when $\mathcal{H}_o \gg \sqrt{2}\sigma$, one has $y_o \gg 1$. In this case the Zeeman shift $\Delta\mathcal{H}_o$ by the mean magnetic field is much larger than the broadening $\gamma_{\mathcal{H}} = \Delta\sqrt{2}\sigma$ by the random magnetic field fluctuations. We call this situation the *strong mean field* limit but it can also be viewed as a weak turbulence limit. When $y_o \gg 1$, one can neglect the term $3/4y_o^2 y$ in Eq. (34) and thus obtain

$$\bar{A}_2^{st} \simeq \frac{1}{4}\sum_{q=-1}^{q=+1}\frac{1}{\gamma_q}(2-3q^2)\left[\left(1-\frac{3}{2y_o^2}\right)H^{(0)}(\bar{x}_q,\bar{a}_q) + q\frac{\gamma_{\mathcal{H}}}{y_o\gamma_q}H^{(1)}(\bar{x}_q,\bar{a}_q)\right], \tag{40}$$

where the superscript "st" stands for strong.

We remark here that if we keep $\gamma_{\mathcal{H}}$ finite but let $y_o \to \infty$, we recover the longitudinal turbulence case discussed in the preceding section. This can be checked on Eqs. (38) to (40).

4.1.2. Weak mean field limit

We now consider the case where $y_o \ll 1$. This means that the Zeeman shift by the mean field satisfies $\Delta\mathcal{H}_o \ll \gamma_{\mathcal{H}}$. Since $\gamma_{\mathcal{H}} < \gamma_1$, this condition automatically implies that the mean Zeeman shift is smaller than the combined Doppler and Zeeman broadening. Thus in this limit, which we refer to as *weak mean field limit*, the mean magnetic field is too weak for the σ-components to be resolved. The best method to obtain the mean absorption coefficients is to start from Eq. (30) and expand the exponentials $\exp(-y_o^2)$ and $\exp(2y_o y)$ in powers of y_o. Using the change of variables described in Appendix C with $y_o = 0$, one obtains at the leading order,

$$\bar{A}_2^{w} \simeq y_o^2\frac{1}{5}\left[H^{(0)}(x,a) - \frac{1}{\gamma_1^6}\left[H^{(0)}\left(\frac{x}{\gamma_1},\frac{a}{\gamma_1}\right) + 2\gamma_{\mathcal{H}}^2 H^{(2)}\left(\frac{x}{\gamma_1},\frac{a}{\gamma_1}\right) + \frac{4}{3}\gamma_{\mathcal{H}}^4 H^{(4)}\left(\frac{x}{\gamma_1},\frac{a}{\gamma_1}\right)\right]\right], \tag{41}$$

where the superscript "w" stands for weak. The important point is that $\bar{A}_2^{w}$ is of order y_o^2. This point has already been made in DP72 and DP79 but the full expression was not given.

For the functions $\bar{A}_0$ and $\bar{A}_1$, the expansion in powers of y_o yields

$$\bar{A}_0^{w} \simeq \frac{1}{3}\sum_{q=-1}^{q=+1}\frac{1}{\gamma_q^3}\left[H^{(0)}\left(\frac{x}{\gamma_q},\frac{a}{\gamma_q}\right) + 2q^2\gamma_{\mathcal{H}}^2 H^{(2)}\left(\frac{x}{\gamma_q},\frac{a}{\gamma_q}\right)\right], \tag{42}$$

$$\bar{A}_1^{w} \simeq \frac{2y_o\gamma_{\mathcal{H}}}{\gamma_1^4}\left[H^{(1)}\left(\frac{x}{\gamma_1},\frac{a}{\gamma_1}\right) + \frac{2}{3}\gamma_{\mathcal{H}}^2 H^{(3)}\left(\frac{x}{\gamma_1},\frac{a}{\gamma_1}\right)\right]. \tag{43}$$

Note that $\bar{A}_1^{w}$ is proportional to $y_o\gamma_{\mathcal{H}}$, i.e. to the shift $\Delta\mathcal{H}_o$ by the mean magnetic field.

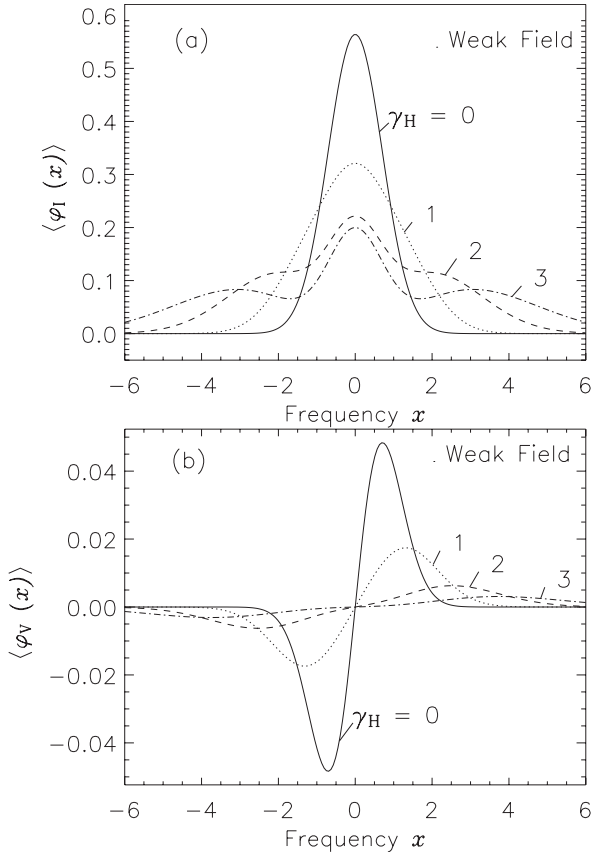

Fig. 3. Weak mean field limit. Isotropic fluctuations. Absorption coefficients $\langle\varphi_I\rangle$ and $\langle\varphi_V\rangle$ for a longitudinal mean magnetic field are shown. Mean Zeeman shift $\Delta\mathcal{H}_o = 10^{-1}$; Voigt parameter $a = 0$. The curve $\gamma_\mathcal{H} = 0$ corresponds to a constant magnetic field equal to $\mathcal{H}_o$.

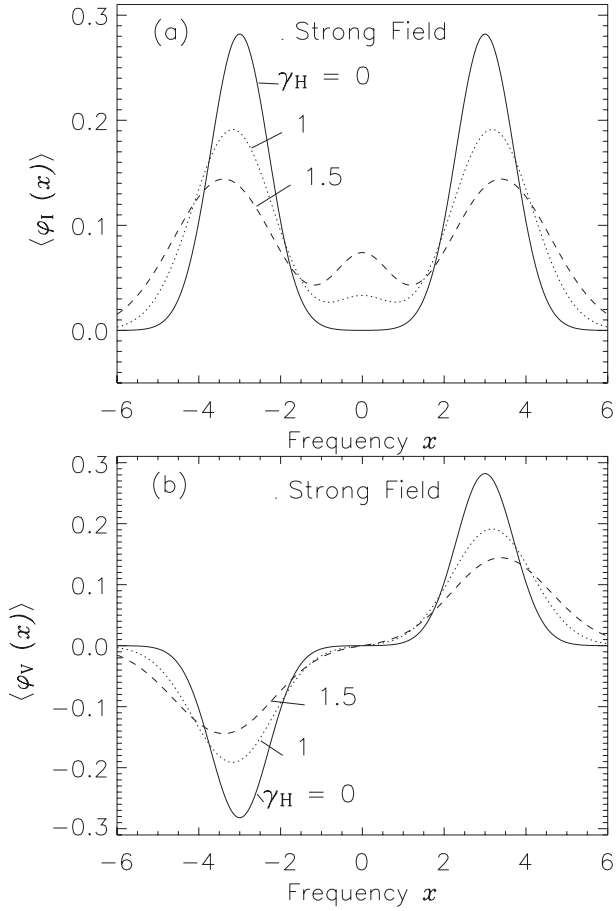

Fig. 4. Strong mean field limit. Isotropic fluctuations. Absorption coefficients $\langle\varphi_I\rangle$ and $\langle\varphi_V\rangle$ for a longitudinal mean magnetic field ($\theta_o = 0°$) are shown. Mean Zeeman shift $\Delta\mathcal{H}_o = 3$; Voigt parameter $a = 0$.The curve $\gamma_\mathcal{H} = 0$ corresponds to a constant magnetic field equal to $\mathcal{H}_o$.

In this weak field limit the mean value of the absorption coefficient φ_I is simply given by $\langle\varphi_I\rangle \simeq \bar{A}_0^w$ since the contribution from $\bar{A}_2^w$, which is of order y_o^2, can be neglected. Thus $\langle\varphi_I\rangle$ is independent of the direction of the mean field. This property holds also when the mean field is constant. The proof given here is an alternative to the standard method which relies on a Taylor series expansion of the Voigt function (Jefferies et al. 1989; Stenflo 1994; LL04).

When the total broadening of the line is controlled by Doppler broadening, i.e. when $\gamma_\mathcal{H} = \Delta\sqrt{2}\sigma \ll 1$, one can set $\gamma_1 = 1$. Equations (42) and (43) lead to the standard results $\varphi_I \simeq H(x,a)$ and $\varphi_V \simeq 2\Delta\mathcal{H}_o H^{(1)}(x,a) = -\Delta\mathcal{H}_o \partial H^{(0)}(x,a)/\partial x$.

4.1.3. Zero mean field

When the mean magnetic field is zero, the angular averaging over Θ and Ψ (or θ and ϕ in the original variables) becomes independent of the averaging over the magnitude of the magnetic field. Because of the isotropy assumption, $\bar{A}_1 = \bar{A}_2 = 0$ and the polarization is zero, namely $\langle\varphi_{Q,U,V}\rangle = 0$ and $\langle\chi_{Q,U,V}\rangle = 0$. The diagonal absorption coefficient is given by $\langle\varphi_I\rangle = \bar{A}_0^w$ with $\bar{A}_0^w$ equal to the rhs of Eq. (42). One can verify that our result is identical to the last equation in Sect. 9.25 of LL04. There $\langle\varphi_I\rangle$ is written in terms of the second order derivative of the Voigt function.

4.2. Profiles of the mean opacity coefficients in the weak and strong mean field limits

In Figs. 3 to 5 we show the effects of an isotropic distribution with a non zero mean field on the absorption and anomalous dispersion coefficients $\varphi_{I,Q,V}$ and $\chi_{Q,V}$. We discuss separately the weak and strong field limits. The results are presented for the damping parameter $a = 0$.

4.2.1. Weak mean field profiles

In the weak mean field limit, $\langle\varphi_I\rangle = \bar{A}_0^w$, up to terms of order y_o^2, $\langle\varphi_V\rangle = \bar{A}_1^w \cos\theta_o$, up to terms of order y_o^3, and $\langle\varphi_Q\rangle$ which is order of y_o^2 can be neglected. As already mentioned above, $\langle\varphi_I\rangle$ is independent of the mean field direction. We show in Fig. 3 the profiles of $\langle\varphi_I\rangle$ and $\langle\varphi_V\rangle$ for $\theta_o = 0°$ calculated with $\Delta\mathcal{H}_o = 10^{-1}$ and $\gamma_\mathcal{H} = 1, 2, 3$. With this choice of parameters, we satisfy the weak mean field condition since $y_o = \Delta\mathcal{H}_o/\gamma_\mathcal{H}$ stays smaller than unity. As can be observed in Fig. 3a the increase of $\gamma_\mathcal{H}$ produces two different effects on $\langle\varphi_I\rangle$. There is a global decrease in amplitude due to the factor $1/\gamma_1^3$ in front of the square bracket in Eq. (42) and the appearance of two shoulders created by the increasing contribution of the term

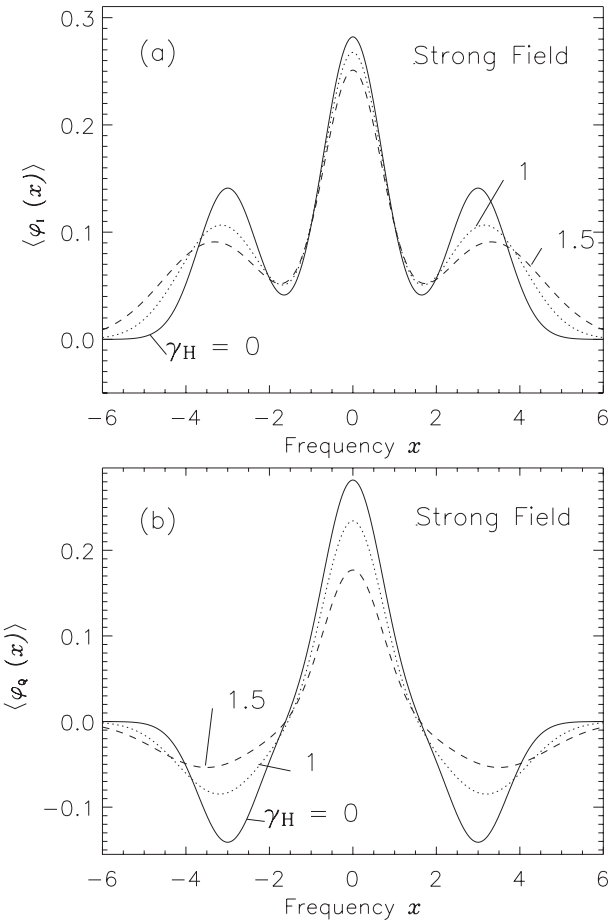

Fig. 5. Strong mean field limit. Isotropic fluctuations. Mean values of $\langle\varphi_I\rangle$ and $\langle\varphi_Q\rangle$ for a transverse mean magnetic field ($\theta_o = 90°$). Same parameters as in Fig. 4 ($\Delta\mathcal{H}_o = 3$; $a = 0$).

with $H^{(2)}$. They are clearly visible for $\gamma_\mathcal{H} = 3$. The position and amplitude of these shoulders can be deduced from the behavior of $H^{(2)}$. Equation (37) shows that the $H^{(n)}$ have maxima at $x^{(n)}_{max} = \pm\sqrt{n/2}$. A rescaling of frequency by the factor γ_1, predicts that the position of these shoulders is around $|x| \simeq \gamma_1$ and their amplitude around $(\gamma^2_\mathcal{H}/\gamma^3_1)(4/3e\sqrt{\pi})$, in agreement with the numerical results. These shoulders are a manifestation of the σ-components which appear with increasing probability when $\gamma_\mathcal{H}$, i.e. the dispersion σ of the random magnetic field, increases.

4.2.2. Strong mean field profiles

In this limit $\langle\varphi_{I,Q,V}\rangle$ are given by Eq. (16) with $\bar{A}_0$, $\bar{A}_1$ given by the exact expressions in Eqs. (38), (39) and $\bar{A}_2$ given by the approximate relation (40). Thus errors that can be created by this approximation will all come from $\bar{A}_2$ and affect only $\langle\varphi_Q\rangle$ and to a lesser extent than $\langle\varphi_I\rangle$. For $\langle\varphi_V\rangle$ we are using an exact expression. Figures 4 and 5 illustrate the variations of $\langle\varphi_I\rangle$, $\langle\varphi_Q\rangle$ and $\langle\varphi_V\rangle$ with the parameter $\gamma_\mathcal{H}$. To satisfy the strong field condition ($y_o = \Delta\mathcal{H}_o/\gamma_\mathcal{H} \gg 1$), we have chosen $\Delta\mathcal{H}_o = 3$ and kept $\gamma_\mathcal{H}$ smaller than 1.5. The variations of $\langle\varphi_I\rangle$ are more easy to understand if we expand the sums over q in Eqs. (38) and (40). This gives

$$\begin{aligned}\langle\varphi_I\rangle \simeq\ & \frac{1}{3}H(x,a)\Big[1-\frac{1}{2}(3\cos^2\theta_o-1)\Big(1-\frac{3}{2y_o^2}\Big)\Big]\\ &+\frac{1}{3\gamma_1}\Big[H(\bar{x}_{+1},\bar{a})+H(\bar{x}_{-1},\bar{a})\Big]\\ &\times\Big[1+\frac{1}{4}(3\cos^2\theta_o-1)\Big(1-\frac{3}{2y_o^2}\Big)\Big]\\ &+\frac{1}{3}\frac{\gamma_\mathcal{H}}{y_o\gamma_1^2}\Big[H^{(1)}(\bar{x}_{+1},\bar{a})-H^{(1)}(\bar{x}_{-1},\bar{a})\Big]\\ &\times\Big[1+\frac{1}{4}(3\cos^2\theta_o-1)\Big].\end{aligned} \tag{44}$$

To simplify the notation we have used $H^{(0)}(x,a) = H(x,a)$, $\bar{a}_{\pm1} = \bar{a}$ and $\bar{a}_0 = a$.

The term containing $H(x,a)$ creates a central component even when the mean field is longitudinal ($\theta_o = 0°$). The existence of this central component, which has no polarization counterpart, was pointed out in DP72. It is created by the averaging of the π-component opacity $\varphi_0 \sin^2\theta/2$ over the isotropic random magnetic field distribution. When $\theta_o = 0°$, this central component behaves as $H(x,a)/2y_o^2$. It becomes clearly visible when $\gamma_\mathcal{H} = 1.5$ (i.e. $y_o = 2$). In Fig. 4 it increases with $\gamma_\mathcal{H}$ because we are keeping the product $y_o\gamma_\mathcal{H} = \Delta\mathcal{H}_o$ constant. When $\theta_o = 90°$, this component behaves as $(1 - 1/2y_o^2)H(x,a)/2$. As can be seen in Fig. 5, it is not very sensitive to the value of $\gamma_\mathcal{H}$.

The σ-components come mainly from the second term in Eq. (44). They vary like $(1 - 1/2y_o^2)H(\bar{x}_{\pm1},\bar{a})/2\gamma_1$ for $\theta_o = 0°$ and as $(1+1/2y_o^2)H(\bar{x}_{\pm1},\bar{a})/4\gamma_1$ for $\theta_o = 90°$. Thus, an increase in $\gamma_\mathcal{H}$ produces a broadening of the components and a decrease in intensity. There is also a shift away from line center more specifically due to the increase of the relative importance of the $H^{(1)}$ terms with respect to the H terms.

The mean coefficients $\langle\varphi_V\rangle$ and $\langle\varphi_Q\rangle$ are given by $\langle\varphi_V\rangle = \bar{A}_1\cos\theta_o$ and $\langle\varphi_Q\rangle \simeq \bar{A}_2^{st}\sin^2\theta_o\cos2\phi_o$ with $\bar{A}_1$ and $\bar{A}_2^{st}$ given in Eqs. (39) and (40). The profiles shown in Figs. 4 and 5 are easy to understand. The dominant contributions come from the terms with $H^{(0)}(\bar{x}_q,\bar{a}_q)$, $q = 0,\pm1$. For $\langle\varphi_V\rangle$, the σ-components behave essentially as $(1 - 1/2y_o^2)H^{(0)}(\bar{x}_{\pm1},\bar{a})/2\gamma_1$, i.e. as the σ-components of $\langle\varphi_I\rangle$. Hence their amplitude decreases and their width increases when $\gamma_\mathcal{H}$ increases. For $\langle\varphi_Q\rangle$, the σ-components behave as $-(1 - 3/2y_o^2)H^{(0)}(\bar{x}_{\pm1},\bar{a})/4\gamma_1$ and the central component as $(1 - 3/2y_o^2)H^{(0)}(x,a)/2$, to be compared to $(1 - 1/2y_o^2)H^{(0)}(x,a)/2$ for $\langle\varphi_I\rangle$. Hence as observed in Fig. 5, the central component of $\langle\varphi_Q\rangle$ is more sensitive to the value of $\gamma_\mathcal{H}$ than the central component of $\langle\varphi_I\rangle$.

4.3. General case. Numerical evaluations

We now discuss the behavior of the mean opacity coefficients when $y_o = \mathcal{H}_o/\sqrt{2}\sigma$ is of order unity. For $\bar{A}_0$ and $\bar{A}_1$ we have exact expressions given in Eqs. (38) and (39) but there is nothing similar for $\bar{A}_2$. Roughly, the weak field limit is valid for $y_o < 0.1$ to 0.2 and the strong field limit for $y_o > 2$. Hence for y_o of order unity, neither the weak nor the strong mean field approximation holds and $\langle\varphi_I\rangle$ and $\langle\varphi_Q\rangle$ must be calculated numerically. For the numerical calculations it is preferable to return

to Eq. (30). The integration over μ can be carried out explicitly. One obtains, for the mean absorption profile,

$$\langle\varphi_I(x,a)\rangle = \frac{4}{3}\frac{1}{\sqrt{\pi}}\,e^{-y_o^2}\int_0^\infty \mathrm{e}^{-y^2}\,y^2\,\sqrt{\frac{\pi}{4y_o y}}$$
$$\Big\{\Big[I_{1/2}(2y_o y) - \frac{1}{2}I_{5/2}(2y_o y)(3\cos^2\theta_o - 1)\Big]H(x,a)$$
$$+\Big[I_{1/2}(2y_o y) + \frac{1}{4}I_{5/2}(2y_o y)(3\cos^2\theta_o - 1)\Big]$$
$$\times\Big[H(x-\gamma_{\mathcal{H}}y,a) + H(x+\gamma_{\mathcal{H}}y,a)\Big]\Big\}\,\mathrm{d}y, \qquad (45)$$

for the mean linear polarization profile

$$\langle\varphi_Q(x,a)\rangle = \sin^2\theta_o\cos 2\phi_o$$
$$\frac{2}{\sqrt{\pi}}\,\mathrm{e}^{-y_o^2}\int_0^\infty \mathrm{e}^{-y^2}\,y^2\,\sqrt{\frac{\pi}{4y_o y}}I_{5/2}(2y_o y)$$
$$\Big\{H(x,a) - \frac{1}{2}[H(x-\gamma_{\mathcal{H}}y,a) + H(x+\gamma_{\mathcal{H}}y,a)]\Big\}\,\mathrm{d}y, \qquad (46)$$

and for the mean circular polarization,

$$\langle\varphi_V(x,a)\rangle = \cos\theta_o\,\frac{4}{\sqrt{\pi}}\,\mathrm{e}^{-y_o^2}\int_0^\infty \mathrm{e}^{-y^2}\,y^2\,\sqrt{\frac{\pi}{4y_o y}}I_{3/2}(2y_o y)$$
$$\frac{1}{2}[H(x-\gamma_{\mathcal{H}}y,a) - H(x+\gamma_{\mathcal{H}}y,a)]\,\mathrm{d}y. \qquad (47)$$

The $I_{l+\frac{1}{2}}$ are the modified spherical Bessel functions of fractional order (Abramovitz & Stegun 1964, p. 443). They have explicit expressions in terms of hyperbolic functions (see Appendix B). In $\langle\varphi_I\rangle$ the terms with $I_{1/2}$ come from $\bar{A}_0$ and the terms with $I_{5/2}$ from $\bar{A}_2$. These expressions are a bit bulky but clearly show the coefficients of the π and σ-components and how they differ from the coefficients in Eq. (5).

The integration over y is performed numerically using a Gauss-Legendre quadrature formula. The integrand varies essentially as $\mathrm{e}^{-y^2}\,\mathrm{e}^{2y_o y}$, with the factor $\mathrm{e}^{2y_o y}$ coming from the Bessel function. The maximum of the integrand is around $y = y_o$. With 10 to 30 points in the range $[0, 2y_o]$ we can calculate the integrals with a very good accuracy (errors around 10^{-6}). The averaging process increases the overall frequency spread of the mean coefficients. A total band width $x_{\max} \approx 4\Delta\mathcal{H}_o$ is adequate to represent the full profiles.

In the following sections we discuss the dependence of $\langle\varphi_I\rangle$ on the intensity of the mean field, on its rms fluctuations and on the damping parameter a. A full section is devoted to $\langle\varphi_I\rangle$ which has the most complex behavior. Then we discuss the dependence of all the mean coefficients, including the anomalous dispersion coefficients, on the Landé factor for a given random magnetic field. All the calculations have been carried out with a damping parameter $a = 0$, except when we consider the dependence on a.

4.4. The mean coefficient $\langle\varphi_I\rangle$

Equation (45) shows that $\langle\varphi_I\rangle$ has a central component around $x = 0$ which corresponds to the π-component. It is of the form $H(x,a)$ times a factor which depends on y_o and on the orientation θ_o of the mean magnetic field. When y_o is small, the Bessel functions can be replaced by their asymptotic expansions around the origin (see Appendix B) and the central component has the approximate expression

$$\langle\varphi_I\rangle_\pi \simeq \mathrm{e}^{-y_o^2}\Big[\frac{1}{3} - \frac{y_o^2}{15}\,(3\cos^2\theta_0 - 1)\Big]H(x,a). \qquad (48)$$

For $y_o = 0$ and $a = 0$ we recover the weak field limit $\langle\varphi_I\rangle_\pi \simeq \mathrm{e}^{-x^2}/3\sqrt{\pi}$. The two other terms in Eq. (45) correspond to the two σ-components, averaged over the random magnetic field. They depend on y_o and θ_o and also on $\gamma_{\mathcal{H}} = \Delta\sqrt{2}\sigma$.

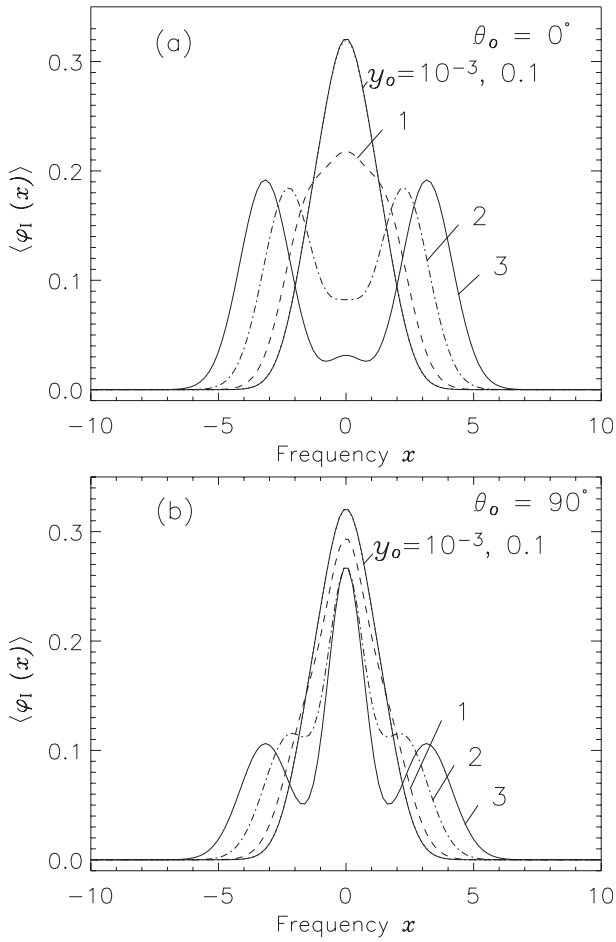

Fig. 6. Dependence of $\langle\varphi_I\rangle$ on the mean magnetic field intensity measured by the parameter y_o. Isotropic fluctuations. The parameters employed are: $a = 0$, $\gamma_{\mathcal{H}} = 1$. The curves for $y_o = 10^{-3}$ and 0.1 coincide. The panels **a)** and **b)** correspond to the longitudinal ($\theta_o = 0°$) and transverse ($\theta_o = 90°$) cases, respectively.

4.4.1. Dependence on the mean magnetic field intensity

We show $\langle\varphi_I\rangle$ in Fig. 6 for different values of y_o. We keep $\gamma_{\mathcal{H}} = 1$, hence $\Delta\mathcal{H}_o = y_o$. We cover all the regimes of magnetic splitting from the weak field regime for $y_o < 0.1$ to the strong field regime for $y_o > 2$. These two regimes have been discussed in Sects. 4.1 and 4.2. For $y_o < 0.1$ there is a single central peak described by the $H^{(0)}$ terms in Eq. (42). There is essentially no contribution from the term with $H^{(2)}$. For $y_o = 1$, one is in the intermediate regime described by Eq. (45). There is still a

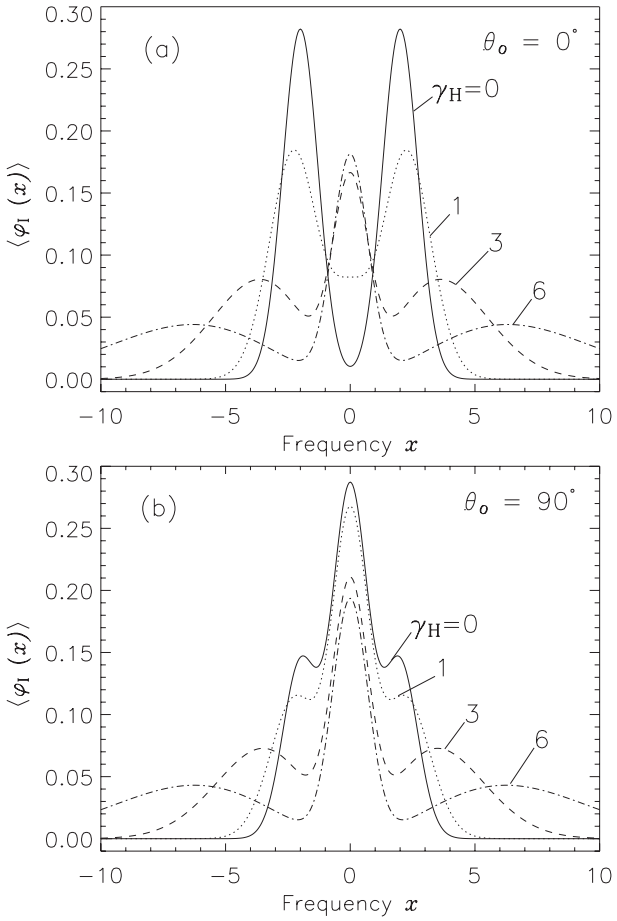

Fig. 7. Dependence of $\langle\varphi_I\rangle$ on the magnetic field dispersion measured by $\gamma_{\mathcal{H}}$. Isotropic fluctuations. The parameters employed are : $a = 0$, $\Delta\mathcal{H}_o = 2$. The panels **a)** and **b)** correspond to longitudinal ($\theta_o = 0°$) and transverse ($\theta_o = 90°$) cases respectively. Notice the saturation of the central π-component for $\gamma_{\mathcal{H}} > 3$.

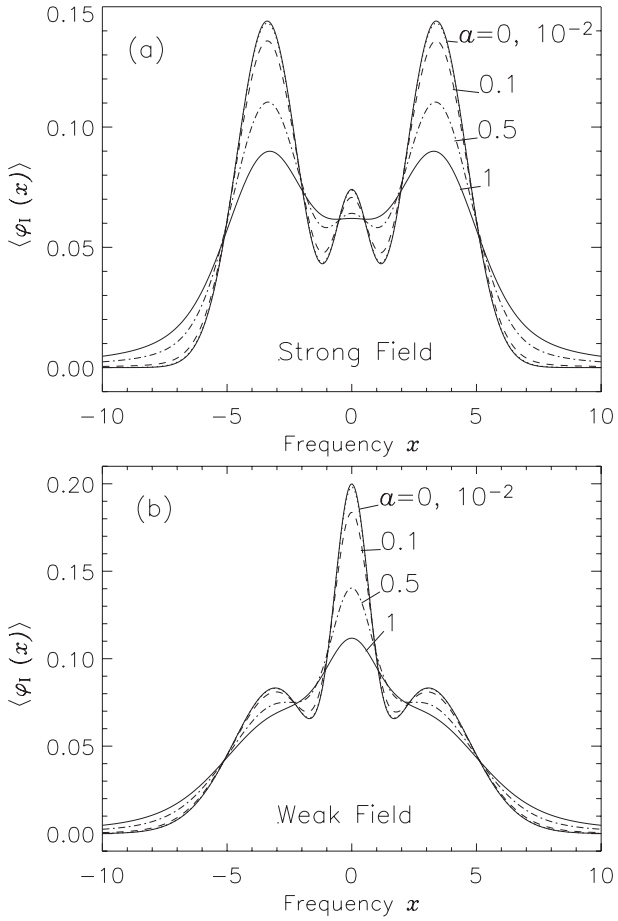

Fig. 8. Dependence of $\langle\varphi_I\rangle$ on the damping parameter a in the $\theta_o = 0°$ case. Isotropic fluctuations. Panel **a)** shows the strong field case ($\Delta\mathcal{H}_o = 3$ and $\gamma_{\mathcal{H}} = 1.5$) and panel **b)** the weak field case ($\Delta\mathcal{H}_o = 10^{-3}$ and $\gamma_{\mathcal{H}} = 3$). For large values of a, the π and σ-components decrease in strength.

single peak because the Zeeman shift $\Delta\mathcal{H}_o = 1$ is smaller than the broadening parameter $\gamma_1 = \sqrt{2}$. Once $y_o > 2$, one enters in the strong field regime, with well separated σ-components at $x = \pm\Delta\mathcal{H}_o = \pm y_o$, discussed in detail in Sect. 4.2.2. When $y_o \to \infty$ while $\gamma_{\mathcal{H}}$ is kept finite, the isotropic distribution goes to the 1D distribution. In the longitudinal case ($\theta_o = 0°$), the central component goes then to zero and the σ-components to $H(\bar{x}_{\pm 1}, \bar{a})/2\gamma_1$, while in the transverse case ($\theta_o = 90°$), they go to $H(x, a)/2$ and $H(\bar{x}_{\pm 1}, \bar{a})/4\gamma_1$, respectively.

4.4.2. Dependence on the magnetic field dispersion

Figure 7 shows $\langle\varphi_I\rangle$ for a fairly strong mean magnetic splitting $\Delta\mathcal{H}_o = 2$ and several values of $\gamma_{\mathcal{H}}$ varying from 0 to 6. For $\gamma_{\mathcal{H}} = 0$ we are in the deterministic case with two well separated σ-components at $x = \pm\Delta\mathcal{H}_o = \pm 2$. Their amplitudes are $H(\Delta\mathcal{H}_o, a)/2$ and $H(\Delta\mathcal{H}_o, a)/4$ for $\theta_o = 0°$ and $\theta_o = 90°$, respectively. The π-component for $\theta_o = 90°$ has an amplitude $H(0, a)/2 = 1/2\sqrt{\pi}$ since $a = 0$. For $\gamma_{\mathcal{H}} = 1$, we are still in the strong field regime ($y_o = 2$) with σ-components still roughly at $x = \pm\Delta\mathcal{H}_o$ but the peaks have smaller intensity because of the factor $1/\gamma_1$ in Eq. (44). For $\gamma_{\mathcal{H}} = 3$, one starts entering into the weak field regime which has been discussed in Sect. 4.2.1 since the corresponding value of y_o is 2/3.

4.4.3. Dependence on the damping parameter

Figure 8 shows $\langle\varphi_I\rangle$ for the longitudinal Zeeman effect. Panel (a) is devoted to the strong mean field regime (see also Fig. 4) and panel (b) to the weak field regime (see also Fig. 3). As long as $a < 10^{-2}$, there are no observable effects on the mean value of φ_I. The effects of the damping parameter on $\langle\varphi_I\rangle$ become noticeable when $a > 0.1$. As expected, the intensity of the π and σ-components decrease and Lorentzian wings appear. When $a > 0.5$, the central component in the strong field case almost disappears. Thus for values of $a \approx 10^{-3}$ to 0.1, the π and σ-components are insensitive to changes in a and the effects of turbulence discussed in this paper for $a = 0$ survive. In the solar case, this situation will hold except for very strong lines.

4.5. Dependence on the Landé factor

We now consider the effect of a given random magnetic field on lines with different Zeeman sensitivities. We give $\boldsymbol{\mathcal{H}}_o$ and

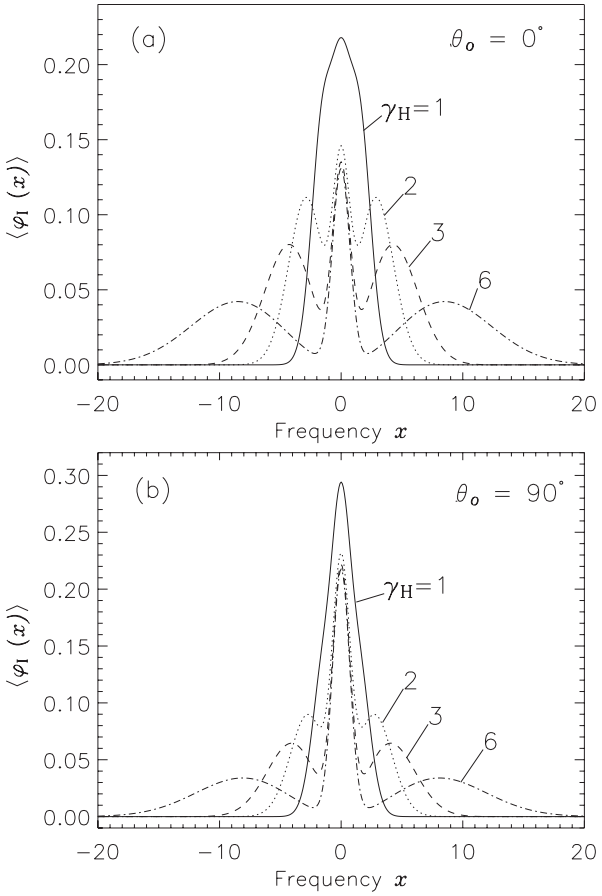

Fig. 9. Dependence of $\langle\varphi_I\rangle$ on the Zeeman sensitivity (the Landé g factor) introduced through the $\gamma_{\mathcal{H}}$ parameter (see the text for details) Isotropic fluctuations. The parameters employed are $a = 0$, and $y_o = 1$. Notice the saturation of the π-component at the line center. The panels **a)** and **b)** correspond to longitudinal ($\theta_o = 0°$) and transverse ($\theta_o = 90°$) cases respectively.

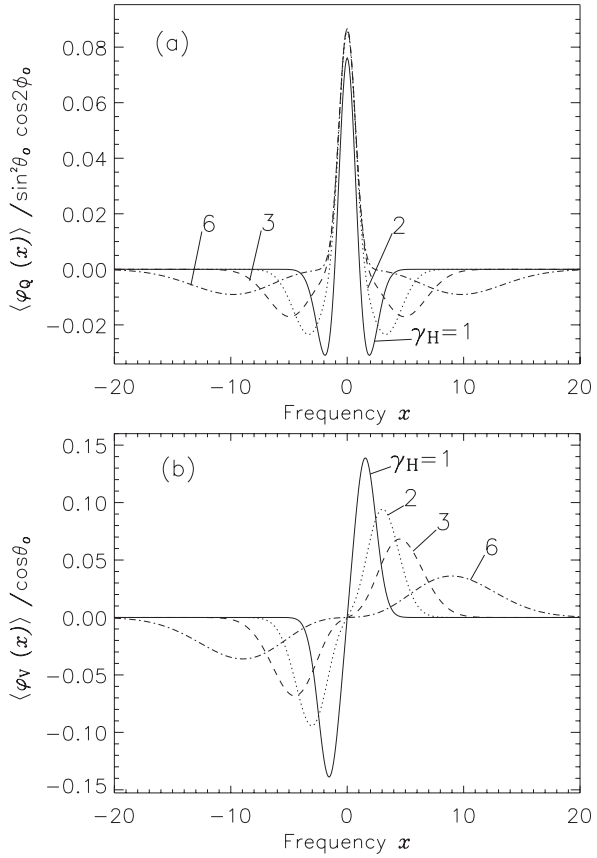

Fig. 10. Same as Fig. 9, but for $\langle\varphi_Q\rangle$ and $\langle\varphi_V\rangle$. The panels **a)** and **b)** correspond to $\langle\varphi_Q\rangle/\sin^2\theta_o \cos 2\phi_o$ and $\langle\varphi_V\rangle/\cos\theta_o$ respectively.

the dispersion σ, but let the Landé parameter g vary. Thus $y_o = \mathcal{H}_o/\sqrt{2}\sigma$ is constant, but $\gamma_{\mathcal{H}} = \Delta\sqrt{2}\sigma$ and $\Delta\mathcal{H}_o = y_o\gamma_{\mathcal{H}}$ are varying with g (see Eq. (8)). The mean coefficients have been calculated with $y_o = 1$ and $\gamma_{\mathcal{H}} = 1$ to 6. For this choice of y_o we are in an intermediate field regime and the mean coefficients are given by Eqs. (45), (46) and (47).

Figure 9 shows $\langle\varphi_I\rangle$. For $\gamma_{\mathcal{H}} = 1$ the Zeeman components are not resolved (the same curve is shown in Fig. 6a, $y_o = 1$). For $\theta_o = 0°$, the central peak is quite broad (Full Width at Half Maximum $FWHM = 5$) because of the superposition of the central π-component coming from the first term in Eq. (45) (responsible for the narrow tip) with the two σ-components given by the two other terms in the same equation. For $\theta_o = 90°$, the central peak is more narrow ($FWHM = 3$), because the contribution from the σ-components is smaller. As can be observed in Eq. (45), the coefficient of $H(x \pm \gamma_{\mathcal{H}} y, a)$ is $(I_{1/2} + \frac{1}{2}I_{5/2})$ for $\theta_o = 0°$ but only $(I_{1/2} - \frac{1}{4}I_{5/2})$ for $\theta_o = 90°$. We recall that the modified Bessel functions are positive functions. When $\gamma_{\mathcal{H}}$ is large enough, the π-component is given by the first term in Eq. (45). It is independent of $\gamma_{\mathcal{H}}$ and its $FWHM$ is around 2. Its amplitude is larger in the transverse than in the longitudinal case since the coefficients of $H(x, a)$ in the integrand are respectively $(I_{1/2} + \frac{1}{2}I_{5/2})$ and $(I_{1/2} - I_{5/2})$. If it were not for the isotropic distribution, there would be no π-component when $\theta_o = 0°$.

The σ-components have essentially the same behavior in the longitudinal and transverse case. The positions of the peaks depend little on θ_o and can be deduced from the position of the maximum of the integrand in Eq. (45). Ignoring the shifted H functions, keeping only the Bessel function of order 1/2 and the positive exponential in the sinh function (see Eq. (B.1)), we find that the maximum is at $y_{max} \simeq (y_o + \sqrt{y_o^2 + 2})/2$. For $y_o = 1$, we get $x_{max} \simeq y_{max}\gamma_{\mathcal{H}} \simeq 1.35\gamma_{\mathcal{H}}$ in fair agreement with the numerical results. The height of the peaks is somewhat larger in the longitudinal than in the transverse case, because the coefficients of the shifted H functions are larger in the first case, as pointed out above.

Figure 10 shows the mean absorption coefficient $\langle\varphi_V\rangle$ divided by $\cos\theta_o$ and $\langle\varphi_Q\rangle$ divided by $\sin^2\theta_o \cos 2\phi_o$ (see Eqs. (47) and (46)). The profile of $\langle\varphi_V\rangle$ is quite standard. As with $\langle\varphi_I\rangle$ the positions of the peaks increase linearly with the Landé factor g and are around $1.35\gamma_{\mathcal{H}}$. For $\langle\varphi_Q\rangle$, the central peak, given by term with $H(x, a)$ is independent of $\gamma_{\mathcal{H}}$, hence it goes to a constant value when the two σ-components are sufficiently far away from line center. This constant value will of course depend on y_o.

Finally, in Fig. 11 we have plotted the mean anomalous dispersion coefficients $\langle\chi_Q\rangle$, divided by $\sin^2\theta_o \cos 2\phi_o$, and $\langle\chi_V\rangle$, divided by $\cos\theta_o$. They are given by Eqs. (46) and (47) with the

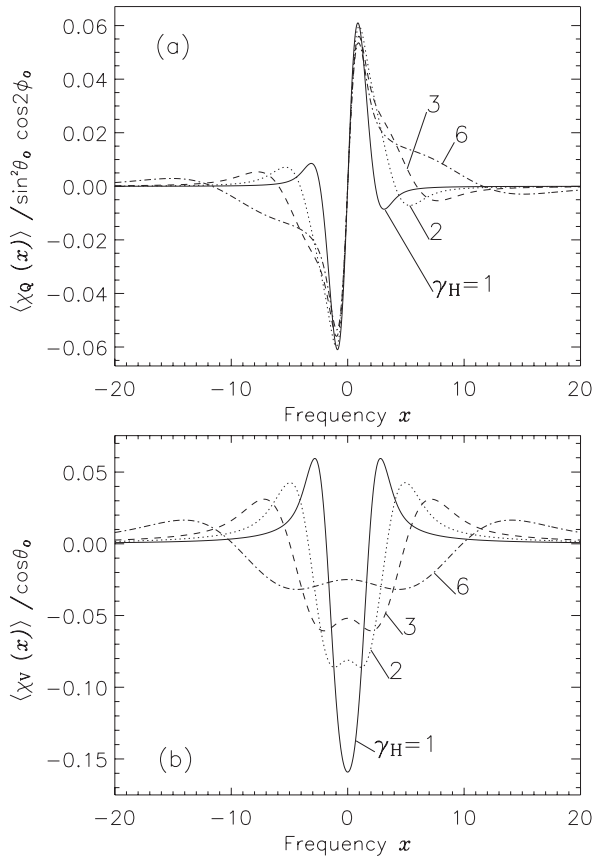

Fig. 11. Dependence of the magneto-optical coefficients $\langle\chi_Q\rangle$ and $\langle\chi_V\rangle$ on the Landé factor. Same model as Fig. 9. Notice the similarity between $\langle\chi_Q\rangle$ and $\langle\varphi_V\rangle$ as well as $\langle\chi_V\rangle$ and $\langle\varphi_Q\rangle$.

Voigt function $H(x, a)$ replaced by the Faraday-Voigt function $F(x, a)$. The coefficient $\langle\chi_Q\rangle$, which has the same symmetry as $\langle\varphi_V\rangle$, keeps more or less the same shape as the Landé factor increases, except for a small broadening long ward of the peaks. This can be explained by considering Eq. (46). The overall shape is controlled by the first term which is independent of $\gamma_{\mathcal{H}}$. The two other terms are responsible for the broadening of the peaks but since they more or less compensate each other around $x = 0$, they do not affect the central part of the profile.

The coefficient $\langle\chi_V\rangle$, has the same symmetries as $\langle\varphi_Q\rangle$ but the opposite sign. Because it involves the difference $F(x - \gamma_{\mathcal{H}}y, a) - F(x + \gamma_{\mathcal{H}}y, a)$ (see Eq. (47)), it is very sensitive to the value of $\gamma_{\mathcal{H}}$ and hence to the Landé factor. For $\gamma_{\mathcal{H}} \geq 3$, one clearly recognizes the shapes of two shifted Dawson integrals with opposite signs in Fig. 11b.

5. Fluctuations perpendicular to the mean field (2D turbulence)

We now assume that the fluctuations of the magnetic field are confined to a plane perpendicular to the direction of the mean field $\boldsymbol{\mathcal{H}}_o$. Integrating over the longitudinal component in Eq. (1), we get the distribution function

$$P_T(\boldsymbol{\mathcal{H}})\,d\boldsymbol{\mathcal{H}} = \frac{1}{(2\pi)\,\sigma^2}\exp\left[-\frac{H_T^2}{2\sigma^2}\right]\mathcal{H}_T\,d\mathcal{H}_T\,d\Psi, \tag{49}$$

where $\mathcal{H}_T$ is the amplitude of the magnetic field in the plane perpendicular to $\boldsymbol{\mathcal{H}}_o$ and Ψ its azimuthal angle in this plane. To simplify the notation we have set $\sigma_T = \sigma$. We recall that $\langle\mathcal{H}_T^2\rangle = 2\sigma^2$. The random field $\boldsymbol{\mathcal{H}}$ is the sum of the mean field $\boldsymbol{\mathcal{H}}_o$ and the fluctuations $\boldsymbol{\mathcal{H}}_T$. Its amplitude satisfies

$$\mathcal{H}^2 = \mathcal{H}_T^2 + \mathcal{H}_o^2. \tag{50}$$

Using Eq. (50) and introducing the dimensionless variables defined in Eq. (19), we can rewrite the 2D distribution function as

$$P_T(\boldsymbol{\mathcal{H}})\,d\boldsymbol{\mathcal{H}} = \frac{1}{\pi}\,e^{-(y^2-y_o^2)}\,y\,dy\,d\Psi, \tag{51}$$

where y varies from y_o to $+\infty$. Equation (17) with $\cos\Theta = \mathcal{H}_o/\mathcal{H} = y_o/y$ leads to

$$\bar{A}_0 = \frac{2}{3}\sum_{q=-1}^{q=+1}\int_{y_o}^{\infty} e^{-(y^2-y_o^2)}H(x - q\gamma_{\mathcal{H}}y, a)y\,dy, \tag{52}$$

$$\bar{A}_1 = y_o\sum_{q\pm1} q\int_{y_o}^{\infty} e^{-(y^2-y_o^2)}H(x - q\gamma_{\mathcal{H}}y, a)\,dy, \tag{53}$$

$$\bar{A}_2 = \frac{1}{4}\sum_{q=-1}^{q=+1}(2-3q^2)\int_{y_o}^{\infty} e^{-(y^2-y_o^2)}H(x - q\gamma_{\mathcal{H}}y, a) \times\left(3\frac{y_o^2}{y^2} - 1\right)y\,dy. \tag{54}$$

When $y_o \to 0$, i.e. when the mean magnetic field is zero, $\bar{A}_1 = 0$ and thus $\langle\varphi_V\rangle$ is also zero. In contrast, $\bar{A}_2$ and hence the mean linear polarization coefficients $\langle\varphi_Q\rangle$ and $\langle\varphi_U\rangle$ are not zero.

5.1. Exact and approximate expressions for the mean coefficients

As shown in DP79, closed form expressions of $\bar{A}_0$ and $\bar{A}_1$ can be obtained in terms of the error function when the damping parameter $a = 0$. For $\bar{A}_2$ approximate expressions can be obtained for $y_o \gg 1$ and $y_o \ll 1$. These different expressions are easily deduced from Eqs. (52) to (54). We give them below together with the weak mean field limits for $\bar{A}_0$ and $\bar{A}_1$. They will be used to analyze the effects of 2D turbulence. Equations (52) and (53) lead to

$$\bar{A}_0 = \frac{1}{3}\left[\frac{1}{\sqrt{\pi}}e^{-x^2} + \frac{1}{\gamma_1^2}\sum_{q=\pm1}\frac{1}{\sqrt{\pi}}e^{-(x-q\Delta\mathcal{H}_o)^2} + 2x\frac{\gamma_{\mathcal{H}}}{\gamma_1^2}\frac{1}{y_o}\bar{A}_1\right], \tag{55}$$

with

$$\bar{A}_1 = y_o\frac{1}{2\gamma_1}e^{y_o^2}e^{-x^2/\gamma_1^2}\sum_{q=\pm1} q\,\mathrm{erfc}\left(y_o\gamma_q - qx\frac{\gamma_{\mathcal{H}}}{\gamma_q}\right), \tag{56}$$

where erfc is the standard complementary error function (Abramovitz & Stegun 1964). If the erfc function is approximated by a Gaussian, one can regroup the exponentials,

and their product behaves as $\exp[-(x-q\Delta\mathcal{H}_o)^2]$, i.e. as a shifted Gaussian (we have used $y_o\gamma_H = \Delta\mathcal{H}_o$). Thus in contrast with 3D and 1D turbulence, there is little broadening of the σ-components by the turbulent magnetic field and the positions of the σ-components will be almost independent of $\gamma_{\mathcal{H}}$.

When $y_o \gg 1$, one has the approximation

$$\bar{A}_2^{\rm str} \simeq \frac{e^{-x^2}}{2\sqrt{\pi}}\left(1-\frac{3}{2y_o^2}\right) -\frac{y_o}{4\gamma_1}e^{y_o^2}e^{-x^2/\gamma_1^2}\sum_{q=\pm1}\mathrm{erfc}\left(y_o\gamma_q - qx\frac{\gamma_{\mathcal{H}}}{\gamma_q}\right)\cdot \quad (57)$$

The first term is obtained by an asymptotic expansion for large x, of the the integrand in Eq. (54) and the second one by assuming $y \simeq y_o$ in the term $(3y_o^2/y^2 - 1)y$. The factor $3/2y_o^2$ is not present in the expansion given in DP79. This factor is needed to explain the π-component observed in Fig. 15.

The combination of Eqs. (55), (56) and (57) with Eq. (16), yields an expression of $\langle\varphi_I\rangle$ for large values of y_o. It contains a term proportional to e^{-x^2}, which yields the central component, and terms which are exactly or approximately of the form $e^{-(x-q\Delta\mathcal{H}_o)^2}$ which determine the σ-components.

In the weak mean field limit, i.e. when $y_o \ll 1$, we have, to leading order,

$$\bar{A}_0^{\rm w} \simeq \frac{1}{3}\left[\frac{2+\gamma_1^2}{\gamma_1^2}\frac{1}{\sqrt{\pi}}e^{-x^2} + 2x\frac{\gamma_{\mathcal{H}}}{\gamma_1^3}e^{-x^2/\gamma_1^2}\mathrm{erf}\left(x\frac{\gamma_{\mathcal{H}}}{\gamma_1}\right)\right], \quad (58)$$

$$\bar{A}_1^{\rm w} \simeq \frac{y_o}{\gamma_1}e^{-x^2/\gamma_1^2}\mathrm{erf}\left(x\frac{\gamma_{\mathcal{H}}}{\gamma_1}\right), \quad (59)$$

$$\bar{A}_2^{\rm w} \simeq -\frac{1}{4\gamma_1^2}\left[\gamma_{\mathcal{H}}^2\frac{1}{\sqrt{\pi}}e^{-x^2} - x\frac{\gamma_{\mathcal{H}}}{\gamma_1}e^{-x^2/\gamma_1^2}\mathrm{erf}\left(x\frac{\gamma_{\mathcal{H}}}{\gamma_1}\right)\right]. \quad (60)$$

The corrections are $O(y_o^2)$ for $\bar{A}_0$ and $\bar{A}_2$ and $O(y_o^3)$ for $\bar{A}_1$. If the erf function is approximated by a Gaussian, its product with e^{-x^2/γ_1^2} yields e^{-x^2}. This implies that broadening by 2D turbulence will be weak.

When the mean field is zero, $\bar{A}_1 = 0$ and $\bar{A}_0$ and $\bar{A}_2$ are given by the rhs in Eqs. (58) and (60) which become exact results.

5.2. Mean absorption profiles for 1D, 3D and 2D turbulence

We compare in Figs. 12 to 15, the mean absorption coefficients corresponding to 1D, 2D and 3D turbulence. Figure 12 corresponds to a weak mean field limit and the other figures to an intermediate regime, neither weak nor strong, with $y_o = 1$. In each figure we also show the absorption coefficients corresponding to a non-random field equal to the mean field $\boldsymbol{\mathcal{H}}_o$. It will be seen that the frequency profiles of the mean coefficients are very sensitive to the nature of the turbulent fluctuations. However there are a few common features linked to the invariance of the frequency integrated mean coefficients (see Sect. 2.4). In particular a broadening (narrowing) of the profile is associated to a decrease (increase) in the peak intensity.

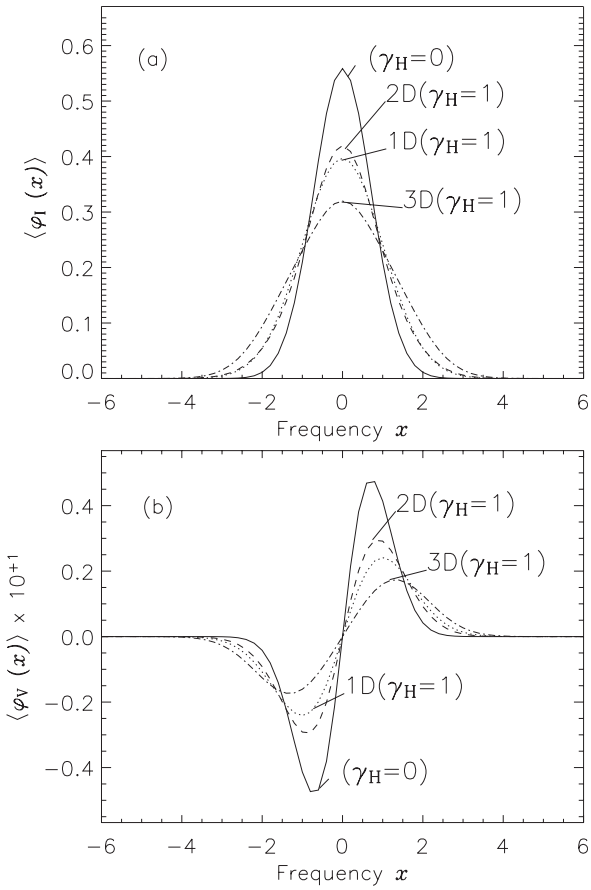

Fig. 12. Dependence of $\langle\varphi_I\rangle$ and $\langle\varphi_V\rangle$ on the magnetic field distribution in the weak mean field limit for the longitudinal Zeeman effect ($\theta_o = 0°$). The model parameters are $a = 0$, $\Delta\mathcal{H}_o = 0.1$ and $\gamma_{\mathcal{H}} = 1$ (hence $y_o = 0.1$). The curves with $\gamma_{\mathcal{H}} = 0$ correspond to a constant magnetic field equal to $\boldsymbol{\mathcal{H}}_o$.

In Fig. 12, $y_o = \Delta\mathcal{H}_o/\gamma_{\mathcal{H}} = 0.1$ is much smaller than the broadening parameter $\gamma_1 = (1+\gamma_{\mathcal{H}}^2)^{1/2} = \sqrt{2}$. Hence $\langle\varphi_I\rangle$ shows a single central peak. The random fluctuations produce a decrease in the peak intensity and an associated broadening. The decrease in peak intensity is the largest for 3D turbulence and the smallest for 2D turbulence. This can be explained with equations established in the previous sections.

For 1D fluctuations and $\theta_o = 0$, we have (see Eq. (27)),

$$\langle\varphi_I\rangle_{\rm 1D}^{\rm w} \simeq \frac{1}{\gamma_1}H\left(\frac{x}{\gamma_1},\frac{a}{\gamma_1}\right)\cdot \quad (61)$$

For 2D turbulence,

$$\langle\varphi_I\rangle_{\rm 2D}^{\rm w} \simeq \frac{2+\gamma_{\mathcal{H}}^2}{2\gamma_1^2}\frac{1}{\sqrt{\pi}}e^{-x^2}, \quad (62)$$

around the line center (see Eqs. (58) and (60)). For isotropic turbulence (see Eq. (42)) we can neglect the contribution of $\bar{A}_2$, which is $O(y_o^2)$. Hence, $\langle\varphi_I\rangle^{\rm w}$ reduces to $\bar{A}_0$, and we have

$$\langle\varphi_I\rangle_{\rm 3D}^{\rm w} \simeq \frac{1}{3}\left[H^{(0)}(x,a) + \frac{2}{\gamma_1}H^{(0)}\left(\frac{x}{\gamma_1},\frac{a}{\gamma_1}\right) + 4\gamma_{\mathcal{H}}^2H^{(2)}\left(\frac{x}{\gamma_1},\frac{a}{\gamma_1}\right)\right]. \quad (63)$$

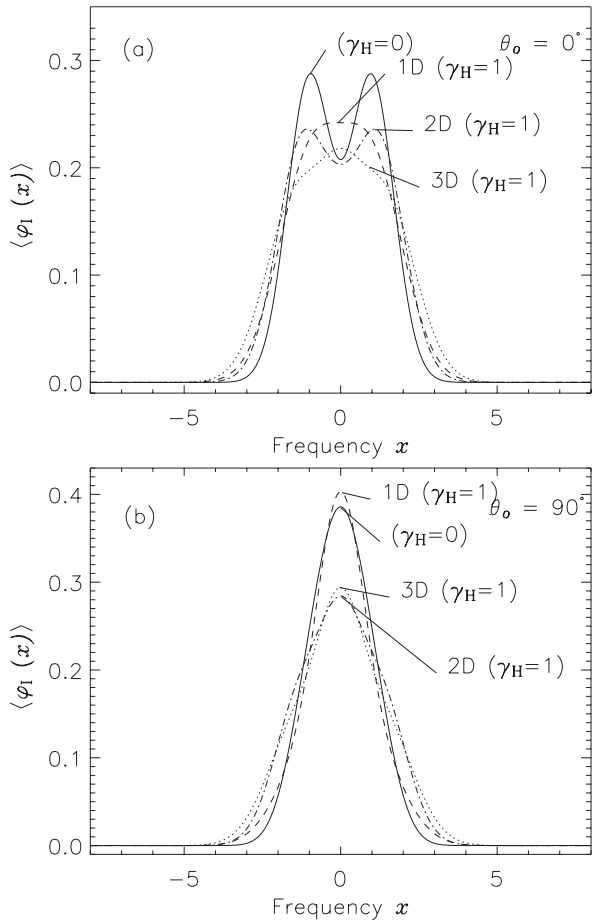

Fig. 13. Dependence of $\langle\varphi_I\rangle$ on the magnetic field distribution. The model parameters are $a = 0$, $\Delta\mathcal{H}_o = 1$, $\gamma_{\mathcal{H}} = 1$ (hence $y_o = 1$). The curves with $\gamma_{\mathcal{H}} = 0$ correspond to a constant magnetic field equal to $\boldsymbol{\mathcal{H}}_o$. Panels **a)** and **b)** correspond to longitudinal ($\theta_o = 0°$) and tranverse ($\theta_o = 90°$) cases, respectively.

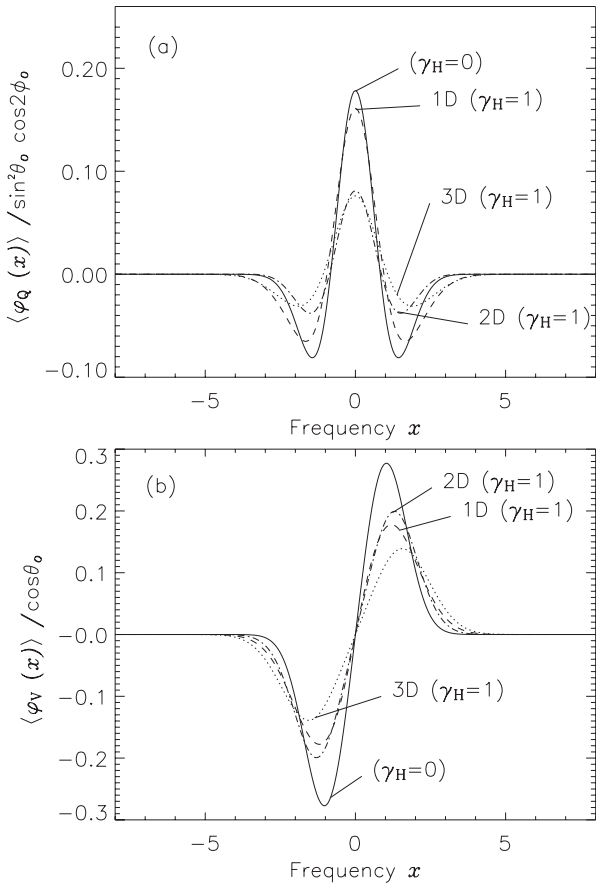

Fig. 14. Dependence of $\langle\varphi_Q\rangle$ and $\langle\varphi_V\rangle$ on the magnetic field distribution. Same model parameters as in Fig. 13. Panels **a)** and **b)** correspond to transverse ($\theta_o = 90°$) and longitudinal ($\theta_o = 0°$) cases, respectively.

The contribution of the term with $H^{(2)}$ is negligible when $\gamma_{\mathcal{H}} = 1$, but becomes relevant when $\gamma_{\mathcal{H}} = 2$, creating pseudo σ-components at $|x| \simeq \gamma_1$ as in Fig. 3. One can verify that the above expressions correctly predict the profiles shown in Fig. 12.

For circular polarization, $\langle\varphi_V\rangle = \bar{A}_1^{\rm w}$, with $\bar{A}_1^{\rm w}$ given in Eqs. (26), (43) and (59) for 1D, 3D and 2D turbulence, respectively. The peak intensity is the largest for 2D turbulence and the smallest for isotropic turbulence (see Fig. 12b), exactly as observed for $\langle\varphi_I\rangle$. The frequencies of the $\langle\varphi_V\rangle$ peaks are at $|x| = 1/\sqrt{2}$ for zero turbulence, around $|x| \simeq \gamma_1/\sqrt{2} = 1$ for 1D turbulence and further away from line center for isotropic turbulence because of the contribution of the term with $H^{(3)}$ (see the discussion in Sect. 4.2.1). For 2D turbulence, numerical simulations show that the maxima are around $|x| \simeq 1$ with not much dependence on the value of $\gamma_{\mathcal{H}}$. This result is suggested in Sect. 5.1.

We now discuss Figs. 13 and 14 where $\Delta\mathcal{H}_o = 1$ and $\gamma_{\mathcal{H}} = 1$. In the non-random case, the two σ-components of the φ_I profile are partially separated when $\theta_o = 0°$ but form a single peak with the π-component when $\theta_o = 90°$. Panel (a) shows that the central frequencies are quite sensitive to the angular distribution of the random field. For 1D turbulence there is a strong broadening of the σ-components which fill up the depression at line center. For 2D turbulence, the σ-components are still well marked but have a smaller intensity. As pointed out above, the broadening of the σ-components is small in the 2D case. For isotropic turbulence, there is also a single broad peak (the same profile is shown in Fig 9, panel (a)). Panel (b), in Fig. 13, corresponds to $\theta_o = 90°$. We note that 2D and 3D turbulence have essentially the same effects. The decrease in the central peak intensity comes from the angular averaging over $\sin^2\theta$. In contrast, the profile is left almost unaffected in the 1D case because the main contribution to the central peak comes from the π-component which is insensitive to the fluctuations of the random field intensity.

Figure 14, panels (a) and (b) show $\langle\varphi_Q\rangle$ and $\langle\varphi_V\rangle$ respectively. We see that $\langle\varphi_Q\rangle / \sin^2\theta_o \cos 2\varphi_o = \bar{A}_2$ behaves in much the same way as $\langle\varphi_I\rangle$ for $\theta_o = 90°$. For 1D turbulence, the central peak is not significantly affected for the reason given above. The σ-components on the other hand suffer some broadening, which goes together with a decrease in intensity. For 2D and 3D turbulence there is a sharp drop in the central peak and also in the σ-components, but the broadening with 2D turbulence is, as already pointed out, much smaller than with 3D turbulence For $\langle\varphi_V\rangle (= \bar{A}_1)$, the fluctuations of the magnetic field produce a decrease in the peak intensity, a small shift away from line

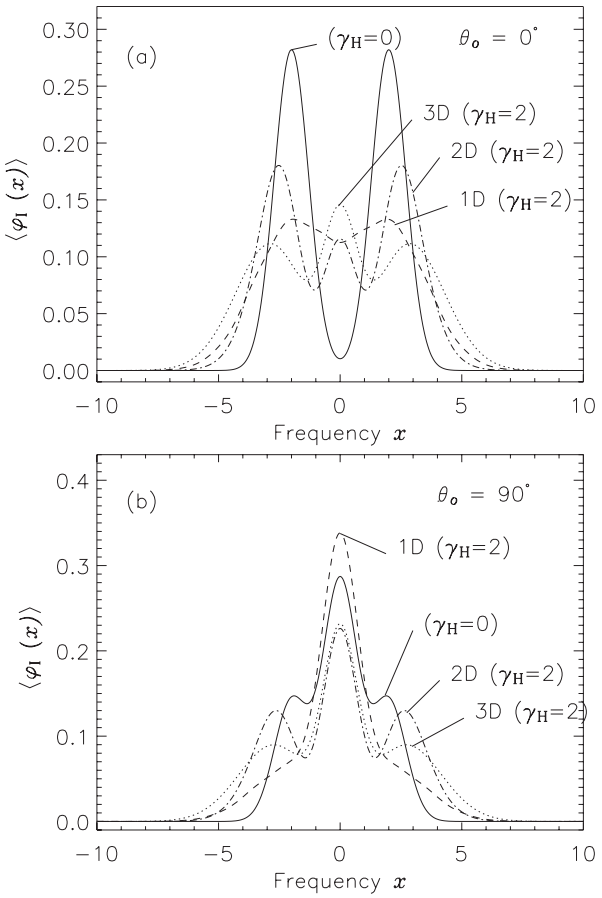

Fig. 15. Dependence of $\langle\varphi_I\rangle$ on the magnetic field distribution. The model parameters are $a = 0$, $\Delta\mathcal{H}_o = 2$, $\gamma_{\mathcal{H}} = 2$ (hence $y_o = 1$). The curves with $\gamma_{\mathcal{H}} = 0$ correspond to a constant magnetic field equal to $\boldsymbol{\mathcal{H}}_o$. Panels **a)** and **b)** correspond to longitudinal ($\theta_o = 0°$) and tranverse ($\theta_o = 90°$) cases, respectively.

center and a broadening which has its largest value for 3D and its smallest value for 2D. The strongest effect is produced by isotropic fluctuations. The decrease in the peak intensity can be explained by the factor $(1 - 1/2y_o^2)$ in Eq. (39).

When the rms fluctuations increase, i.e. when $\gamma_{\mathcal{H}}$ increases, the profiles $\langle\varphi_Q\rangle$ and $\langle\varphi_V\rangle$ keep essentially the same shape but the effects are amplified. All the peaks have a smaller intensity and for 2D and 3D turbulence the σ-components are moved away further from line center. One also observes a significant decrease in the slope of $\langle\varphi_V\rangle$ at line center.

In Figs. 15 we still have $y_o = 1$, (rms fluctuations equal to the mean field intensity) but $\Delta\mathcal{H}_o = 2$ and $\gamma_{\mathcal{H}} = 2$. Hence the σ-components are well separated as can be observed. Panel (a) of this figure clearly shows the central component created by the averaging of π-component over the random directions of the magnetic field for 2D and 3D turbulence. For 2D turbulence, the σ-components are significantly more intense and more narrow than for 3D turbulence. The central peak on the other hand is shallower. For 1D turbulence, there is no central component but a strong broadening of the σ-components. The decrease in the intensity of the σ-components is controlled by the factor $1/\gamma_1 \simeq 1/\sqrt{5} \simeq 0.44$ (see Eq. (22)). For the transverse case (panel (b)), the σ-components disappear for 1D turbulence because they are multiplied by $1/\gamma_1$ but the central peak increases due to the contribution of the broadened σ-components. This increase of the central peak can also be understood in terms of the constancy of the frequency integral of $\langle\varphi_I\rangle$. For 2D and 3D turbulence, the σ-components are still well marked but they are somewhat shifted away from line center with the 3D components being broader and shallower than the 2D components. The decrease of the central peak is due to the averaging over the $\varphi_o \sin^2\theta/2$ term.

6. Summary and concluding remarks

In this paper we have examined the effects of a random magnetic field on the Zeeman line transfer propagation matrix. We have considered a fairly general case where the magnetic field has anisotropic but azimuthally invariant Gaussian fluctuations about a given mean magnetic field $\boldsymbol{\mathcal{H}}_o$ which can be set to zero. We have examined in detail three types of random fluctuations : (i) longitudinal fluctuations which take place along the direction of the mean field; referred to as 1D or longitudinal turbulence; (ii) fluctuations which are distributed isotropically around the direction of the mean field referred to as isotropic or 3D turbulence; (iii) fluctuations isotropically distributed in a plane perpendicular to the mean field, referred to as 2D turbulence; the total random field (sum of the fluctuating part and of the mean field) does not lie in this plane unless the mean field is zero. In all three cases, the random field depends on two parameters, the mean field $\boldsymbol{\mathcal{H}}_o$ and the dispersion σ^2 around the mean field (see Eqs. (18), (28), (49)).

First we give a fairly compact and simple expression for the mean coefficients of the propagation matrix. It is valid for any random field invariant in a rotation around the mean field direction (Eq. (16)). This general expression is obtained by taking advantage of the fact that the angular dependence of the Zeeman matrix elements can be written in terms of the spherical harmonics $Y_{lm}(\theta, \phi)$, where θ and ϕ are the polar and azimuthal angles of the random field with respect to direction of the line of sight.

The random fluctuations of the magnetic field have two types of effects. The fluctuations of the magnetic field strength (modulus) produce random Zeeman shifts which lead to a broadening of the σ-components. It is important to note that the π-component is not affected by this phenomenon. The second effect, which occurs only for 2D and 3D turbulence, is the averaging over the angular dependence of the coefficients which affects both the π and σ-components. As a result, the frequency profiles of the mean coefficients can look quite different from the standard profiles created by a constant magnetic field. The physically relevant parameters for the analysis of the mean profiles are the dimensionless parameters y_o, which measures the intensity of the mean magnetic field $\boldsymbol{\mathcal{H}}_o$ in units of the rms fluctuations σ, and $\gamma_{\mathcal{H}}$, the Zeeman shift by the rms fluctuations. The Zeeman shift by the mean magnetic field is $\Delta|\boldsymbol{\mathcal{H}}_o| = y_o\gamma_{\mathcal{H}}$. The broadening by the magnetic field intensity fluctuations combined with the standard Doppler broadening (by thermal and/or microturbulent velocity fluctuations) is described by a parameter $\gamma_1 = (1 + \gamma_{\mathcal{H}}^2)^{1/2}$. There are two interesting limiting regimes. A *weak mean field* regime

corresponding to $\Delta|\boldsymbol{\mathcal{H}}_o| \ll \gamma_1$, i.e. to a Zeeman shift by the mean magnetic field smaller than the combined Doppler and magnetic broadening. The other interesting limit, referred to as the *strong mean field* or *weak turbulence* regime, corresponds to $y_o \gg 1$. In this limit, the σ-components stay well separated in spite of the random field fluctuations, provided γ_1 stays smaller than y_o. We now briefly summarize the main effects for the three types of fluctuations that we have considered.

For 1D turbulence, the direction of the random magnetic field remains constant and same as the direction (θ_o, ϕ_o) of the mean magnetic field. The only effect is a broadening and a decrease in intensity by a factor γ_1 of the σ-components (see Sect. 3. and Figs. 12 to 15). For the transverse Zeeman effect ($\theta_o = 90°$) and when $y_o \simeq 1$, a consequence of this broadening is that the central π-component can be enhanced by the magnetic field fluctuations while the σ-components almost entirely disappear (see Fig. 15). When the intensity of the mean magnetic field is zero, the coefficient of circular polarization $\langle\varphi_V\rangle$ (and $\langle\chi_V\rangle$) are zero but not the mean linear polarization coefficients $\langle\varphi_Q\rangle$ and $\langle\varphi_U\rangle$. Circular polarization is destroyed by fields of opposite directions but not linear polarization which has a quadratic dependence on the polar angle of the magnetic field.

For isotropic (3D) turbulence, the two effects namely, magnetic broadening of the σ-components and angular averaging are at work. The dependence of the absorption and anomalous dispersion coefficient profiles on the magnetic field parameters and on the Landé factor is discussed in detail in Sect. 4. One striking effect in the case of the longitudinal Zeeman effect ($\theta_o = 0°$) is the formation in $\langle\varphi_I\rangle$ of a central component with no polarization counterpart created by the averaging of $\varphi_0 \sin^2\theta/2$. This component is particularly noticeable when $y_o \simeq 1$ (see Figs. 9 and 15). The circular polarization coefficients $\langle\varphi_V\rangle$ (and $\langle\chi_V\rangle$) can be expressed in terms of generalized Voigt and Faraday-Voigt functions $H^{(n)}$ and $F^{(n)}$. The other mean coefficients can also be expressed in terms of these generalized functions but only in weak mean field and strong mean field regimes. When the mean magnetic field is zero, the random field $\boldsymbol{\mathcal{H}}$ is strictly isotropic (there is no preferred direction) and both circular $\langle\varphi_V\rangle$ and linear $\langle\varphi_Q\rangle$ and $\langle\varphi_U\rangle$ polarization coefficients are zero. The same is true of course for the anomalous dispersion coefficients.

For 2D turbulence the mean profiles resemble the mean profiles for isotropic turbulence. One can observe in particular the formation of a non-polarized central component due to the averaging of $\varphi_o \sin^2\theta/2$ over the directions of the random field, but in contrast to isotropic turbulence, there is very little broadening of the σ-components because the magnitude of the random field is more centered around the magnitude of the mean field. The σ-components are not only more narrow they are also stronger than with 1D or 3D turbulence (see the figures in Sect. 5). When the mean magnetic field is zero, the mean circular polarization coefficient $\langle\varphi_V\rangle$ is zero but not the linear coefficients $\langle\varphi_Q\rangle$ and $\langle\varphi_U\rangle$. So even if the mean magnetic field is zero, anisotropic turbulence like 1D or 2D turbulence will produce linear polarization.

In this work we have considered for simplicity a normal Zeeman triplet. In the anomalous Zeeman splitting case, each elementary component φ_q ($q = 0, \pm 1$) must be replaced by a weighted average of the form

$$\bar{\varphi}_q = \sum_{M_u} H_q(x_q, a) S_q(M_l, M_u), \quad q = M_l - M_u, \tag{64}$$

where S_q is the strength of the transition between the lower and upper levels of magnetic quantum numbers M_l and M_u and $x_q = x - (g_l M_l - g_u M_u)\Delta\mathcal{H}$, with $\mathcal{H}$ the intensity of the random magnetic field (Stenflo 1994). The absorption and anomalous dispersion coefficients can still be written as in Eqs. (10) and (11) with the φ_q replaced by $\bar{\varphi}_q$ and the summation now over M_u. Similarly, the mean coefficients are given by Eq. (16) where the $\bar{A}_i$ are now calculated with the $\bar{\varphi}_q$. The exact and approximate expressions given for 1D, 2D and 3D turbulence can thus be carried over to the anomalous Zeeman splitting.

Here we have considered only Gaussian distributions but it is clear that the averaging method and the main effects that we have described will carry over to other types of distributions. Such effects as the broadening of the σ-components by random Zeeman shifts or the appearance of unpolarized central components due to angular averaging should persist. The assumption that the random fields are azimuthally symmetric plays an important role in the averaging method, but is a fairly realistic assumption for small scale fluctuations. As for correlations between magnetic and velocity fluctuations, they can certainly be incorporated in the averaging method without major difficulties.

For weak lines (optical depth small compared to unity), the opacity coefficients give a fair approximation to the observable Stokes parameters and a comparison between observations and mean coefficient profiles could provide informations on the statistical properties of the magnetic field. For example, the intensity of the mean magnetic field could be obtained with the center-of-gravity method (see e.g. LL04, p. 640). This method is based on the measurements of the center of gravity wavelength $x_\pm$. For weak lines, they can be written as

$$x_\pm = \frac{\int(\langle\varphi_I\rangle \pm \langle\varphi_V\rangle)x\,\mathrm{d}x}{\int(\langle\varphi_I\rangle \pm \langle\varphi_V\rangle)\,\mathrm{d}x}, \tag{65}$$

where the frequency integration is extended to the full line profile. As $\langle\varphi_V\rangle$ is antisymmetric with respect to line center, $\langle\varphi_I\rangle$ symmetric and normalized to unity, Eq. (65) reduces to

$$x_\pm = \pm \int \langle\varphi_V\rangle x\,\mathrm{d}x. \tag{66}$$

Using Eqs. (11), (16) and (17), one obtains

$$x_\pm = \pm\cos\theta_o\Delta \int \mathcal{H}\cos\Theta P(\boldsymbol{\mathcal{H}})\,\mathrm{d}\boldsymbol{\mathcal{H}}, \tag{67}$$

where Θ is the angle between the random field $\boldsymbol{\mathcal{H}}$ and the mean field $\boldsymbol{\mathcal{H}}_o$. Hence $\mathcal{H}\cos\Theta$ is the longitudinal component of the random field. The integration over the magnetic field distribution given in Eq. (1) leads to

$$x_\pm = \pm\cos\theta_o\Delta\mathcal{H}_o, \tag{68}$$

hence to a measure of the longitudinal component $\mathcal{H}_o\cos\theta_o$ of the mean magnetic field.

A detailed analysis of Stokes profiles for lines with different Zeeman sensitivity (Landé factors) would be a way to evaluate the dispersion of the random fluctuations. The detection of an unpolarized central component in Stokes I would indicate strong variations in the direction of the magnetic field. However, specific observations at high resolution would be required to verify this fact, because a central unpolarized component may also be produced by a non-magnetic region within the resolution element.

For spectral lines with moderate to large optical depths, radiative transfer effects must be taken into account. The Unno-Rachkovsky solution shows very large differences in the observable Stokes parameters, depending on whether the magnetic field is random or not. This topic will be addressed in subsequent papers where we consider random magnetic fields with a finite correlation length.

Acknowledgements. M.S. is financially supported by Council of Scientific and Industrial Research (CSIR), through a Junior Research Fellowship (JRF Grant No.: 9/890(01)/2004-EMR-I). This support for the Research work is gratefully acknowledged. She would like to thank the Director, Indian Institute of Astrophysics (IIA) and JAP program, for providing excellent research facilities. Further K.N.N. and M.S. are grateful to the Laboratoire Cassiopée (CNRS), the PNST (CNRS) and the French Ministère de l'Éducation Nationale for financial support during a visit at the Observatoire de la Côte d'Azur where part of this work was completed. H.F. was supported by the Indo-French Center for the Promotion of Advanced Research (IFCPAR 2404-2) and by the Indian Institute of Astrophysics during her visits to Bangalore. She would like to thank Dr. V. Bommier for stimulating discussions. The authors are grateful to the referee for constructive remarks.

References

Abramovitz, M., & Stegun, I. 1964, Handbook of Mathematical functions, App. Math. Ser., 55 (National Bureau of Standards)

Brink, D. M., & Satchler, G. R. 1968, Angular Momentum, 2nd edition (Oxford: Clarendon Press)

Cattaneo, F. 1999, ApJ, 515, l39

Cattaneo, F., Emmonet, T., & Weiss, N. 2003, ApJ, 588, 1183

Dolginov, A. Z., & Pavlov, G. G. 1972, Soviet Ast., 16, 450 (transl. from Astron. Zh., 49, 555, 1972)

Dolginov, A. Z., Gnedin, Yu. N., & Silant'ev, N. A. 1995, Propagation and Polarization of Radiation in Cosmic Media (Gordon and Breach Publishers)

Domke, H., & Pavlov, G. G. 1979, Ap&SS, 66, 47

Faurobert-Scholl, M. 1996, Sol. Phys., 164, 79

Heinzel, P. 1978, Bull. Astron. Inst. Czechosl, 29, 159

Hui, A. K., Armstrong, B. H., & Wray, A. A. 1978, J. Quant. Spec. Radiat. Transf., 19, 509

Janßen, K., Vögler, A., & Kneer, F. 2003, A&A, 409, 1127

Landi Degl'Innocenti, E. 1976, A&AS, 25, 379

Landi Degl'Innocenti, E. in ASP Conf. Ser. 307, ed. J. Trujillo Bueno, & J. Sánchez Almeida, 593

Landi Degl'Innocenti, E., & Landolfi, M. 2004, Polarization in Spectral Lines (Kluwer Academic Publishers)

Matta, F., & Reichel, A. 1971, Math. Comput. 25, 339

Rees, D. E. 1987, in Numerical Radiative Transfer, ed. W. Kalkofen, 213 (Cambdrige University Press)

Sánchez Almeida, J. 1997, ApJ, 491, 993

Sánchez Almeida, J., Landi Degl'Innocenti, E., Martinez Pillet, V., & Lites, B. W. 1996, ApJ, 466, 537

Sánchez Almeida, J., & Lites, B. W. 2000, ApJ, 532, 1215

Socas-Navarro, H., & Sánchez Almeida J. 2003, ApJ, 593, 581

Stenflo, J. O. 1982, Sol. Phys., 80, 209

Stenflo, J. O. 1994, Solar Magnetic Fields (Kluwer Academic Publishers)

Stenflo, J. O., & Holzreuter, R. 2002a, in Current Theoretical Models and Future High Resolution Solar observations: Preparing for ATST, ed A. A. Pevtsov, & H. Uitenbroek, ASP Conf. Ser. 286, 169

Trujillo Bueno, J., Shchukina, N., & Asensio Ramos, A. 2004, Nature, 430, 326

Varshalovich, D. A., Moskalev, A. N., & Khersonskii, V. K. 1988, Quantum Theory of Angular Momentum (World Scientific)

Online Material

Appendix A: Some properties of the Wigner rotation matrices $D^{(l)}_{mm'}$ and spherical harmonics Y_{lm}

The properties that are needed here can be found in Brink & Satchler (1968, Appendix IV), Varshalovich et al. (1988) or in LL04. We reproduce them here for convenience.

The Wigner matrices $D^{(l)}_{mm'}(\alpha,\beta,\gamma)$ ($l \geq 0$, $-l \leq m,m' \leq +l$) are the transformation matrices for irreducible tensors of rank l in rotations of the reference frame. The angles α,β,γ are the Euler angle of the rotation. The $D^{(l)}_{mm'}$ have an explicit representation:

$$D^{(l)}_{mm'} = \mathrm{e}^{-im\alpha} d^{(l)}_{mm'}(\beta) \mathrm{e}^{-im'\gamma}, \tag{A.1}$$

where $d^{(l)}_{mm'}(\beta)$ is real. Tables of $d^{(l)}_{mm'}$ can be found in the above references.

The Y_{lm} are special cases of $D^{(l)}_{mm'}$ corresponding to $m' = 0$ (or $m = 0$):

$$\begin{aligned} D^{(l)}_{m0}(\phi,\theta,\gamma) &= \sqrt{\frac{4\pi}{2l+1}}\, Y^*_{lm}(\theta,\phi) \\ &= \sqrt{\frac{4\pi}{2l+1}}\, d^{(l)}_{m0}(\theta) \mathrm{e}^{im\phi}. \end{aligned} \tag{A.2}$$

The Legendre polynomial $P(\theta)$ are special cases of Wigner matrices corresponding to $m = 0$ and $m' = 0$, or in other words, special cases of Y_{lm} corresponding to $m = 0$:

$$P_l(\cos\theta) = D^{(l)}_{00}(\phi,\theta,\gamma) = \sqrt{\frac{4\pi}{2l+1}}\, Y^*_{l0}(\theta,\phi). \tag{A.3}$$

The first Legendre polynomials are

$$P_0(\theta) = 1; \quad P_1(\theta) = \cos\theta; \quad P_2(\theta) = \frac{1}{2}(3\cos^2\theta - 1). \tag{A.4}$$

The Y_{lm} for small l can be found in many reference books (e.g. Brink & Satchler 1968; Varshalovich et al. 1988; Dolginov et al. 1995). In particular

$$Y_{2,\pm 2} = \left(\frac{15}{32\pi}\right)^{1/2} \sin^2\theta\, \mathrm{e}^{\pm 2i\phi}. \tag{A.5}$$

The angular dependence of φ_I, $\varphi_{Q,U}$ and φ_V can thus be expressed in terms of the Y_{lm} (see Eq. (10)). This property is used to calculate their average values over the magnetic field distribution.

Appendix B: Modified spherical Bessel functions

The functions of order 0, 1 and 2 introduced in Eqs. (45), (46) and (47) can be obtained by performing the integration over μ in Eq. (30) (see also Abramovitz & Stegun, 1964, p. 443). They may be written as

$$\sqrt{\frac{\pi}{2z}} I_{1/2}(z) = \frac{1}{z}\sinh z, \tag{B.1}$$

$$\sqrt{\frac{\pi}{2z}} I_{3/2}(z) = -\frac{1}{z^2}\sinh z + \frac{1}{z}\cosh z, \tag{B.2}$$

$$\sqrt{\frac{\pi}{2z}} I_{5/2}(z) = \left(\frac{3}{z^3} + \frac{1}{z}\right)\sinh z - \frac{3}{z^2}\cosh z. \tag{B.3}$$

For small values of z, one has at leading order,

$$\sqrt{\frac{\pi}{2z}} I_{1/2}(z) \simeq 1; \quad \sqrt{\frac{\pi}{2z}} I_{3/2}(z) \simeq \frac{z}{3}; \tag{B.4}$$

$$\sqrt{\frac{\pi}{2z}} I_{5/2}(z) \simeq \frac{z^2}{15}. \tag{B.5}$$

All the functions $\sqrt{\pi/2z} I_{l+1/2}(z)$, for z real and positive, have positive values and go to ∞ as $z \to \infty$.

Appendix C: Integration over Gaussian distributions

The mean values $\bar{A}_i$ are given by the averages, over the magnetic field distributions, of Voigt or Faraday-Voigt functions, multiplied by some polynomials (see Eq. (17)). Explicit expressions for the average values are given in Eq. (22) for 1D turbulence, in Eqs. (38), (39), (40), (41), (42), (43), for 3D turbulence. We show here how to obtain these expressions which for 3D turbulence involve the generalized $H^{(n)}$ (and $F^{(n)}$) functions introduced in Sect. 4.1 and discussed in Appendix D. Several methods are available to carry out the integration. One can consider the Fourier transforms of the quantities to be averaged. One can write the functions $H^{(0)}$ and $F^{(0)}$ as real and imaginary parts of the function $W^{(0)}(z)$, with z complex (see Appendix D) and then do contour integrations in the complex plane. Here we describe a direct method based on simple changes of variables.

The integrals we want to transform are of the form

$$\begin{aligned} B_q = \frac{a}{\pi^{3/2}} \frac{1}{\sqrt{\pi}} \int_{-\infty}^{+\infty} \int_{-\infty}^{+\infty} \frac{\mathrm{e}^{-u^2}}{(x-u-q\gamma_{\mathcal{H}} y)^2 + a^2} \\ \times \mathrm{e}^{-(y_\mathrm{o}-y)^2} P(y)\, \mathrm{d}y\, \mathrm{d}u, \end{aligned} \tag{C.1}$$

where $P(y)$ is a polynomial in y. For 1D turbulence, $P(y) = 1$ (see Sect. 3.). The weak field limit corresponds to $y_\mathrm{o} = 0$.

First we transform the integral over u. We write

$$x - u - q\gamma_{\mathcal{H}} y = t - s, \tag{C.2}$$

with t and s defined by

$$t = x - q\gamma_{\mathcal{H}} y_\mathrm{o}; \quad s = u + q\gamma_{\mathcal{H}}(y - y_\mathrm{o}). \tag{C.3}$$

Note that $t = 0$ gives the positions of the σ-components corresponding to the mean magnetic field $\mathcal{H}_\mathrm{o}$. We thus get

$$\begin{aligned} B_q = \frac{a}{\pi^{3/2}} \frac{1}{\sqrt{\pi}} \int_{-\infty}^{+\infty} \int_{-\infty}^{+\infty} \frac{\mathrm{e}^{-[s-q\gamma_{\mathcal{H}}(y-y_\mathrm{o})]^2}}{(t-s)^2 + a^2} \\ \times \mathrm{e}^{-(y_\mathrm{o}-y)^2} P(y)\, \mathrm{d}y\, \mathrm{d}s. \end{aligned} \tag{C.4}$$

Regrouping the two exponentials, we rewrite

$$\begin{aligned} &[s - q\gamma_{\mathcal{H}}(y - y_\mathrm{o})]^2 + (y_\mathrm{o} - y)^2 = \\ &\quad s^2 + (y - y_\mathrm{o})^2\gamma_1^2 - 2sq\gamma_{\mathcal{H}}(y - y_\mathrm{o}) = \frac{s^2}{\gamma_q^2} + \frac{\zeta^2}{\gamma_q^2}, \end{aligned} \tag{C.5}$$

with

$$\zeta = \gamma_q^2\left[(y - y_o) - q\frac{\gamma_{\mathcal{H}}}{\gamma_q^2}s\right]. \tag{C.6}$$

Thus Eq. (C.4) becomes

$$B_q = \frac{a}{\pi^{3/2}}\frac{1}{\sqrt{\pi}}\int_{-\infty}^{+\infty}\int_{-\infty}^{+\infty}\frac{\mathrm{e}^{-s^2/\gamma_q^2}}{(t-s)^2+a^2} \times \mathrm{e}^{-\zeta^2/\gamma_q^2}\frac{1}{\gamma_q^2}P(y_o + \frac{\zeta}{\gamma_q^2} + q\frac{\gamma_{\mathcal{H}}}{\gamma_q^2}s)\,\mathrm{d}\zeta\,\mathrm{d}s. \tag{C.7}$$

Since P is a polynomial in ζ, the Gaussian integral over ζ can be calculated explicitely and one obtains a polynomial in s. It is easy to see that the integral over s can be expressed as a combination of $H^{(n)}$ functions. When $P(y) = 1$, the integral over ζ, divided by $\sqrt{\pi}$, gives a factor γ_q and one obtains $B_q = H(\bar{x}_q, \bar{a}_q)/\gamma_q$, where $\bar{x}_q$, $\bar{a}_q$ and γ_q are defined in Eqs. (23) and (24).

Appendix D: The functions $H^{(n)}$ and $F^{(n)}$

The functions $H^{(n)}$ and $F^{(n)}$ introduced in Eqs. (35) and (36) of the text are the real and imaginary part of the function

$$W^{(n)}(z) = \frac{i}{\pi^{3/2}}\int_{-\infty}^{+\infty}\frac{u^n\mathrm{e}^{-u^2}}{z-u}\,\mathrm{d}u, \tag{D.1}$$

where $z = x + ia$ is a complex number and n a positive integer. The usual Voigt and Faraday-Voigt functions correspond to $n = 0$. The function $W^{(0)}(z)$ is the complex probability function (Abramovitz and Stegun 1964) also known as the Faddeeva function. We also note that $W(iw) = D(w)$, where $D(w)$ is the complex Dawson function introduced in Heinzel (1978).

The $W^{(n)}$ satisfy a recurrence formula which leads to simple recurrence relations for $H^{(n)}$ and $F^{(n)}$ and thus to a method of calculation. In the numerator of Eq. (D.1), we write $u^n = u^{n-1}(u - z + z)$ and immediately obtain

$$W^{(n)}(z) = zW^{(n-1)}(z) - \frac{i}{\pi^{3/2}}\int_{-\infty}^{+\infty}u^{n-1}\mathrm{e}^{-u^2}\,\mathrm{d}u. \tag{D.2}$$

Separating the real and imaginary parts, we find the two recurrence relations,

$$H^{(n)}(x,a) = xH^{(n-1)}(x,a) - aF^{(n-1)}(x,a), \tag{D.3}$$

$$F^{(n)}(x,a) = xF^{(n-1)}(x,a) + aH^{(n-1)}(x,a) - \frac{1}{\pi^{3/2}}\int_{-\infty}^{+\infty}u^{n-1}\mathrm{e}^{-u^2}\,\mathrm{d}u. \tag{D.4}$$

When n is even, the integral in Eq. (D.4) is zero.

The recurrence relations take very simple forms when the Voigt parameter $a = 0$. For $H^{(n)}$, they lead to Eq. (37) of the text. For $F^{(n)}$, with $n \geq 1$ one has

$$F^{(n)}(x,0) = xF^{(n-1)}(x,0) - \frac{1}{\pi}\frac{1.3\ldots(2k-1)}{2^k}. \tag{D.5}$$

The constant term, where $k = (n-1)/2$, comes from the integral in Eq. (D.4). It is zero for even values of n. For $n = 0$, $F^{(0)}(x,0) = 2D(x)/\pi$, with $D(x)$ the Dawson integral. To calculate this integral we have used the algorithm by Hui et al. (1978).

When a is not zero, $H^{(0)}$ and $F^{(0)}$ have been calculated with the algorithm of Hui et al. (1978) which is more accurate than the algorithm of Matta & Reichel (1971), especially for $F^{(0)}$.

We note that the derivatives of the Voigt and Faraday-Voigt functions can be expressed in terms of the functions $H^{(n)}$ and $F^{(n)}$. For example

$$\frac{\partial H(x,a)}{\partial x} = -2H^{(1)}(x,a), \tag{D.6}$$

$$\frac{\partial^2 H(x,a)}{\partial x^2} = -2H^{(0)}(x,a) + 4H^{(2)}(x,a), \tag{D.7}$$

with identical relations for $F(x,a)$.